Contemporary Mathematics
https://ojs.wiserpub.com/index.php/CM/

Research Article

Method for Solving Fuzzy-Stochastic Diffusive SIR-β Systems: Development and Stability Analysis

Muhammad Shoaib Arif[1*], **Yasir Nawaz**[2]

[1] Department of Mathematics and Sciences, College of Sciences and Humanities, Prince Sultan University, Riyadh, 11586, Saudi Arabia
[2] Department of Mathematics, Faculty of Engineering and Computing, National University of Modern Languages (NUML), Islamabad, 44000, Pakistan
E-mail: marif@psu.edu.sa

Received: 1 November 2025; **Revised:** 8 December 2025; **Accepted:** 26 December 2025

Abstract: This study presents a novel computational framework for deterministic and stochastic models. A computational scheme is constructed on two-time levels. A compact approach is employed to efficiently manage space-dependent terms, with the initial stage utilizing a modified exponential integrator. The stability and consistency of the scheme in the mean-square sense have also been established. The concept is implemented on a stochastic fuzzy diffusive SIR-β model, which is resolved using three distinct numerical techniques. To assess accuracy and performance, a comparative analysis is performed between the proposed scheme and the current Non-Standard Finite Difference (NSFD) scheme. The findings indicate that the proposed system consistently outperforms the NSFD method, ensuring greater numerical stability and precision in epidemic modelling. The comparison shows that the proposed scheme performs better than the existing non-standard finite difference scheme in most cases.

Keywords: exponential integrator scheme, stability and consistency in a mean square sense, SIR-β model, stochastic fuzzy model, diffusion process

MSC: 35R60, 65M06, 65C30

1. Introduction

An essential component of epidemiology, infectious disease modelling addresses patterns of illness transmission and provides data to direct the development of appropriate control strategies. One of the mathematical models applied to examine the dynamics of infectious illness transmission is the Susceptible-Infected-Recovered (SIR) model [1]. Given flaws in epidemiological data, assumptions made by conventional deterministic SIR models concerning parameters and initial conditions may be illogical. Stochastic models and fuzzy-logic approaches have helped reduce these doubts, leading to more robust and flexible disease modelling [2].

The stochastic SIR model is better suited to describe real-world uncertainty, including individual behavioural variability and random environmental fluctuations, by incorporating randomness into the disease transmission and recovery processes. Different populations have different degrees of illness susceptibility; hence, different transmission

DOI: https://doi.org/10.37256/cm.7220269051

rates have also been shown using distribution. Further, showing how diseases spread across areas with varying population densities is the use of diffusion effects, which explain geographical variance.

Dealing with missing or inaccurate data presents one of the most challenging difficulties in epidemiological models. Strong for managing uncertainty and ambiguity, the fuzzy logic approach uses fuzzy numbers rather than exact values to explain epidemiological elements. Examining uncertainty in disease transmission rates, recovery rates, and environmental factors enables the incorporation one stochastic differential equations into fuzzy systems, thereby improving the accuracy of illness predictions.

To better comprehend the issue and make informed decisions, computational engineers use mathematical and statistical models. The first mathematical models of epidemics were published in 1766. Smallpox accounted for one in fourteen deaths in England at this time, and Daniel Bernoulli developed a mathematical model to study it [3]. Vaccination against viruses would add about three years to the life expectancy at birth, according to Bernoulli's model. In [4], you can find the English translation of this book. Kermack et al. [5–7] established the deterministic compartmental epidemic model. Enko analyzed the interactions between infected and susceptible individuals within the community and constructed a probabilistic model to describe the measles epidemic in discrete time [8]. Many models were developed, analyzed, and employed qualitatively and statistically to investigate infectious diseases. To better understand the transmission and treatment of infectious illnesses, and to compare, organize, implement, evaluate, and optimize various detection, prevention, therapeutic, and control programs, mathematical models are invaluable tools.

The immunity of sensitive individuals can prevent numerous infectious diseases, and specific infections can confer temporary or permanent protection against reinfection in recovered patients. Varieties of epidemic models, such as Susceptible, Infected, and Recovered (SIR), Susceptible, Exposed, Infectious, and Recovered (SEIR), and Susceptible, Vaccinated, Exposed, Infectious, and Recovered (SVEIR), have been extensively studied by the scientific community. To better understand the disease's transmission, Olopade et al. [9] investigated an SEIR mathematical model that incorporated treatment rates and natural immunity. Immunity can be acquired through targeted immunization, naturally following complete recovery from infection, or through the transmission of maternal antibodies to the infant, providing partial immunity. The duration of immunity varies with the disease, with some conferring nearly lifelong immunity while others offer only a transient period of resistance. Vaccine-induced immunity often requires a booster after a specific period, particularly when the Vaccine's efficacy diminishes due to insufficient exposure to illness. In measles, vaccinated individuals exhibit inferior immunity compared to those with natural immunity [10, 11]. Scherer and McLean proposed several mass vaccination models that offer essential insights into the expected outcomes of immunization efforts. They demonstrate how to determine the level of immunization coverage needed to eradicate an infection, examine the effects of declining vaccine-induced immunity, and study the interplay between vaccine-sensitive and -resistant strains of infectious agents [12]. In their mathematical model for cholera epidemics, Sanches et al. [13] accounted for seasonality, host immunity decline, and cholera control initiatives. In disease modelling, Jain et al. [14] examined innate immunity.

Zadeh [15] first introduced the concept of fuzzy sets in 1965. Mathematical modelling primarily relies on fuzzy Theory, which facilitates the management of uncertain or ambiguous data within a mathematical framework. Conventional mathematical models assume that every variable is precisely calculable or quantifiable. The model's uncertainty arises because variables in many real-world scenarios may be poorly defined or even impossible to measure. One can better handle ambiguity with the mathematical framework of fuzzy theory, which allows variables to take on values that are not explicitly stated but are indicated by varying degrees of set membership. Since mathematical models enable a more flexible and accurate representation of variables, they can fairly capture the intricate and erratic aspects of real-world systems. The degree to which parameter values in mathematical models are unknown or imprecise is indicated by fuzzy parameters. Fuzzy parameters help handle inaccurate data and intricate interactions among variables. Including expert opinion and subjective data in mathematical models enables the quantitative portrayal of imprecision and ambiguity. Numerous mathematical models have used fuzzy Theory. Mathematical models that use fuzzy Theory improve predictive and assessment capabilities, allowing the researchers to build more robust models that handle uncertainty and imprecision. Epidemic models have been enhanced and refined through numerous applications of fuzzy Theory. Barros et al. [16] and Mondal et al. [17] looked at epidemic models with unknown transmission coefficients in two separate studies. The

Susceptible-Infectious-Recovered-Susceptible (SIRS) model was suggested by Mishra et al. [18] to account for the network-wide uncertainty in worm transmission.

Many classical methods, including forward Euler, Runge-Kutta, and others, can generate oscillations, chaos, and false steady states under certain conditions. The non-standard finite-difference approach can be used to construct schemes that avoid these numerical instabilities. Mickens [19] was an early proponent of this method, and it has since led to new numerical schemes that preserve physical properties such as boundedness, positivity, and stability. Verma et al. pursued the Generalized Burgers-Huxley (GBH) problem using the Non-Standard Finite Difference (NSFD) method [20]. Khalsaraei et al. introduced a technique for NSFD assessment of influenza. We present numerical results and analyze several interesting features of the proposed method [21]. After considering counselling and antiviral medication in their study of a bisexual community, Razza et al. found that the stochastic model of the Human Immunodeficiency Virus (HIV)/Acquired Immunodeficiency Syndrome (AIDS) epidemic is more realistic than the deterministic one.

According to [22], the NSFD stochastic scheme kept all the key features of the disease dynamical model. To better understand the HIV/AIDS epidemic, Jawaz et al. [23] created a model based on NSFD and studied a delayed reaction-diffusion epidemic. Among many other applications, the NSFD Theory put forth by Mickens is widely used in the mathematical and numerical modelling of diseases [24, 25]. Recent advancements in computational epidemiology have introduced robust numerical schemes for simulating stochastic epidemic models, incorporating partial immunity, treatment effects, and fractal-stochastic transport phenomena [26–28]. These developments enhance model realism and numerical accuracy, offering vital tools for understanding complex disease transmission dynamics under uncertainty.

To study the dynamics of the new Coronavirus Disease 2019 (COVID-19), Aslefallah et al. developed the Susceptible-Infective-Treated-Recovered (SITR) model. Conducting an error analysis verifies the model's accuracy [29]. The singular boundary method is applied to the solution of a two-dimensional altered anomalous diffusion process with initial Dirichlet-type boundary conditions and a non-linear source term. To simulate the process using Riemann-Liouville fractional derivatives, they employed a two-dimensional non-linear time-fractional sub-diffusion equation [30]. No matter the geometry of the domain, the two-dimensional telegraph equation may be solved using the Singular Boundary Method (SBM) [31]. Radial point interpolation without a spectral mesh for two-dimensional pseudo-parabolic equations is the subject of this study. The finite difference time-stepping method is used to approximate time derivatives. The convergence and stability of this meshless method are theoretically proven and extensively examined [32]. Allehiany et al. [33] used the NSFD approach to solve a COVID-19 model involving fuzziness numerically. A computer virus model that utilized fuzzy criteria was investigated by Alhebshi et al. [34].

Over the past ten years, it has become clear that epidemic models fail to portray how infectious diseases will behave accurately. There is evidence of non-deterministic behaviour in the collected empirical data on the disease's spread [35]. Thus, several stochastic models have been proposed to model the spread of the disease in human populations. These include stochastic semi-mechanistic models [36], stochastic SIS epidemic models with non-linear incidence rates [37], stochastic SIRS epidemic models with saturated incidence rates [38], and stochastic SIS non-linear stochastic epidemiological models with double epidemic hypothesis and incidence rate [39]. Considering the outbreak in the context of an interruption is a perfectly reasonable thought process.

The numerical investigation of Stochastic Differential Equations (SDEs) is a popular area of research. The stochastic epidemic model was analytically and numerically solved by Cai et al. [40]. A general incidence rate and a time delay are components of the stochastic eco-epidemiological model proposed by Meng et al. The special case of a positive global solution with positive initial circumstances was discussed during their discussion. In addition, they laid the groundwork for the model's stochastic analysis [41]. The authors determined the conditions for eradicating and maintaining the disease by incorporating a stochastic hepatitis B model [42]. The authors of [43] examined the COVID-19 model using numerical methods. The writers used numerical approximations to solve the stochastic partial differential equations [44]. The many dynamics of the stochastic SIR model were examined by Zhao et al. [45]. They prove that there is one unique positive global solution to the model and that, under certain circumstances, the solution oscillates about the equilibrium points. Additional research has also focused on SDEs, which incorporate random effects and uncertainty into dynamical systems. Numerical methods such as Euler-Maruyama, Milstein, and stochastic Runge-Kutta schemes have been widely developed to approximate solutions of SDEs, particularly when analytical solutions are not available. These methods [46–48] ensure

stability and accuracy in capturing the probabilistic behaviour of stochastic processes, making them essential tools in fields such as finance, biology, and fluid dynamics.

There has been significant interest in mathematical models that examine the spread of infectious diseases through human behaviour. According to the modelling principles, there are three main methods for depicting feedback effects in transmission dynamics models. A common approach is to describe the feedback loop between the transmission of a disease and the behavioural response of humans by changing the parameters of compartmental models from constant to variable, typically the transmission term.

Because the effective contact rate β changes over time in this setting, many non-linear functions have been employed to characterize it. As an example, to account for the psychological effect in the population, specifically increased self-protective behaviour at high levels of I, Capasso, and Serio [49] provided a saturated function $\beta(yt) = \frac{\beta_\circ}{1+kI(t)}$, where I is the number of infectious individuals and $\beta_\circ$ is the nominal contact rate.

In [50, 51], the exponential decay function $\beta(t) = \beta_\circ e^{-\alpha_1 E - \alpha_2 I - \alpha_3 H}$ and $\beta(t) = \beta_\circ(1 - e^{-aI})$ were given to illustrate how factors such as social media and mask-wearing affect the likelihood of transmission control, with E representing the exposed population and H the hospital population, respectively. In addition, Xiao et al. [52] presented a piecewise-smooth function that depends on I and its derivative; this function causes a media coverage impact switch on the contact rate. The following studies and their references discuss the use of similar non-linear functions in transmission terms [53–56]. According to research by [57–59], one way to model feedback is to split the population into subpopulations based on individuals' levels of awareness, perceptions of risk, or activity levels.

In particular, Baazeem et al. [57] examined the impact of private and public knowledge on illness dissemination using a SIRS-type model that incorporated private awareness from direct population contacts and public awareness from information efforts. In contrast, Arif et al. [59] created a compartmental model to compare the efficacy of self-imposed measures and government-imposed social distancing in reducing, delaying, or preventing the COVID-19 pandemic. The model was stratified by the population's disease status and awareness. There is also the possibility of describing the pandemic as a two-part dynamical process that interacts with one another: the disease-related compartmental component and the regulatory component [60].

To be more precise, models in this category have been proposed with an additional compartment for factors such as media coverage [61] and a disease-prevalence information index [62], which help uncover the regulatory variable's epidemiological role in behaviour modification.

What is Already Known in the Open Literature: Classical epidemiological models such as SIR and SEIR, and their extensions, have been widely used to study the spread of infectious diseases. Existing numerical methods for such models often focus on either deterministic or stochastic aspects, with limited exploration of fuzzy uncertainties in epidemic parameters. Non-Standard Finite Difference (NSFD) schemes have been applied to preserve positivity and boundedness, but often struggle to accurately capture dynamics under uncertainty and randomness.

What is Missing (Research Gap): Current models do not adequately capture both types of real-world uncertainties: (i) Epistemic uncertainty (parameter imprecision) and (ii) Aleatoric uncertainty (stochastic randomness). There is a lack of robust computational frameworks that can integrate: Fuzzy logic for imprecise epidemic parameters, Stochastic perturbations to represent external random influences, Compact numerical strategies for spatial discretization, and Exponential integrators tailored for stiff stochastic systems.

Novel Contributions: The Fuzzy Stochastic SIR-β model with diffusion effects proposed in this research extends conventional models by combining these methodologies to achieve a more accurate and practical computational framework. This hybrid model can capture stochastic variation and uncertainty in epidemiological parameters while accounting for spatial diffusion, making it highly relevant for real-world epidemic studies. The main objective of this work is to develop a computational method for solving the Fuzzy Stochastic SIR-β model with diffusion effects. The main contributions of this work consist of:

• We developed a computational method capable of solving deterministic and stochastic models, specifically tailored for the fuzzy SIR-β model with diffusion.

• We design the scheme using two time levels to eliminate the need for auxiliary methods at the initial time step, simplifying the computational process.

• Analyzing the impact of fuzzy uncertainty and stochasticity on disease dynamics.

• Be sure the scheme is accurate, for practical reasons, by assessing its consistency and stability in the mean-square sense.

• Evaluate the performance of the proposed scheme against existing non-standard finite difference methods to demonstrate its advantages and effectiveness.

Combining stochastic processes, fuzzy logic, and diffusion systems produces the fuzzy stochastic SIR-β model with diffusion. This hybrid model captures the uncertainty in parameter estimations, the randomness of disease transmission, and the spatial distribution of infections well. Still, tackling this complex model poses significant computational challenges. Conventional numerical methods cannot manage complicated uncertainty and spatial components. Therefore, modern computational systems that effectively and precisely control these challenging aspects are much needed.

Purpose of this Study: The primary purpose of this paper is methodological, not just to solve one specific epidemiological example. More precisely:

1. To develop a new explicit two-stage numerical scheme (predictor-corrector with a modified exponential integrator and sixth-order compact spatial discretization) for non-linear fuzzy-stochastic reaction-diffusion partial differential equations.

2. To establish the theoretical properties of this scheme, in particular, mean-square stability, consistency in the mean-square sense, and resulting convergence of the fully discrete method.

3. To adapt and implement this scheme for a fuzzy stochastic diffusive SIR-β epidemic model with spatial diffusion, dynamic (state-dependent) transmission rate β, fuzzy epidemiological parameters (e.g. μ, δ), and stochastic perturbations modelled by Wiener processes.

4. To compare the proposed method with an NSFD scheme and a reference MATLAB solver (pdepe), to demonstrate the practical advantages in accuracy, stability, and handling of fuzziness and stochasticity in epidemic simulations.

This work presents a deterministic SIR-β model that accounts for variation in the rate of contact resulting from individual behavioural responses, thereby enhancing the conventional Susceptible-Infectious-Removed (SIR) model. By making this adjustment, the model can now capture two-way feedback effects: how changes in behaviour affect the dynamics of the disease, and how disease transmission affects the dynamics of behaviour. The computational and analytical practicality of the model is further enhanced by its suitably simple structure. Essential modelling properties are preserved, and the balance between mathematical representations of complex social and behavioural processes is maintained.

2. Fuzzy set

A function $\delta_A(x)$ that maps the elements from the set X to the unit interval $[0, 1]$ is called a fuzzy set A in X, and it is characterized by a membership function $\lambda_A(x)$. The fuzzy set can be represented as

$$A = \{(x_i, \delta_A(x_i)) : x_i \varepsilon X\} \tag{1}$$

Each element in A is an ordered pair comprised of the element of X and its corresponding image in $[0, 1]$, which tells the grade of membership. The membership function is called a triangular membership function if it is expressed in the form of a triangle, which is represented as

$$\delta_A(x) = \begin{cases} 0 \text{ for } x \leq a_1 \\ \frac{x-a_1}{c_1-a_1} \text{ for } a_1 \leq x \leq c_1 \\ \frac{d_1-x_1}{d_1-c_1} \text{ for } c_1 \leq x \leq d_1 \\ 0 \text{ for } d_1 \leq x \end{cases} \tag{2}$$

3. Proposed fuzzy numerical scheme

Constructing a two-stage predictor-corrector scheme for solving non-linear stochastic partial differential equations involves a systematic approach to handle nonlinearity and randomness effectively. This study focuses on solving partial differential equations with fuzzy parameters. The partial differential equation that contains fuzzy parameters can be written as

$$\frac{\partial u}{\partial t} = \alpha_1 \frac{\partial^2 u}{\partial x^2} + f(u), x\varepsilon[0, L], t\varepsilon[0, T] \tag{3}$$

Where α_1 is a triangular fuzzy number handled via the β_1-cut approach, the function $f(u)$ is a nonlinear source term. The problem is defined in a one-dimensional spatial domain, i.e., $x\varepsilon[0, L]$, where $L > 0$. We consider an initial condition of the form $u(x, 0) = u_\circ(x)$ for $x\varepsilon[0, L]$, where $u_\circ(x)$ is a given fuzzy-valued function satisfying necessary smoothness and compatibility conditions. We impose the Neumann boundary conditions $\frac{\partial u}{\partial t}(0, t) = 0$, $\frac{\partial u}{\partial t}(L, t) = 0$. We confirm that the problem is modelled in a one-dimensional spatial domain, i.e., the function $u(x, t)$ is defined on $x\varepsilon[0, L]$, with diffusion in the x-direction only.

Handling the Fuzzy Parameter Using the β_1-Cut Approach: To manage the fuzziness of α_1, the β_1-cut approach [63] is employed, representing α_1 as an interval $[0.4\beta_1, 3 - \beta_1]$. Eq. (3) can be expressed as a fuzzy differential equation using β_1-cut approach as

$$\frac{\partial}{\partial t}\left[\overleftrightarrow{u}_1(t, x, \beta_1), \overleftrightarrow{u}_2(t, x, \beta_1)\right] = \alpha_1 \frac{\partial^2}{\partial x^2}\left[\overleftrightarrow{u}_1(t, x, \beta_1), \overleftrightarrow{u}_2(t, x, \beta_1)\right] + f\left[\overleftrightarrow{u}_1(t, x, \beta_1), \overleftrightarrow{u}_2(t, x, \beta_1)\right] \tag{4}$$

The Eq. (4) is expressed in two different components $\overleftrightarrow{u}_1$ and $\overleftrightarrow{u}_2$. The scheme is constructed on one part $\overleftrightarrow{u}_1$which is expressed as u.

3.1 *Step-by-step construction of the scheme*

Step 1: Predictor Stage:
The first stage predicts the solution at the next time step using:

$$\overline{u}_i^{n+1} = \frac{1}{2}u_i^n e^{5\Delta t} + \frac{1}{2}u_i^n e^{-4\Delta t} + \left(e^{5\Delta t} + e^{-4\Delta t} - 2\right)\left\{\left.\frac{\partial u}{\partial t}\right|_i^n - \frac{1}{2}u_i^n\right\} \tag{5}$$

Here, superscript n denotes the time level, i.e., $t^n = n\Delta t$, where Δt is the time step, and $n\varepsilon N$ indexes the time level. The subscript i denotes the spatial grid point, i.e., $x_i = i\Delta x$ where Δx is the spatial step size and $i \in \{0, 1, \ldots, N\}$ indexes

the discretized spatial domain. The quantity $\left.\frac{\partial u}{\partial t}\right|_i^n$ represents the partial derivative of u with respect to time, evaluated at the spatial grid point x_i and at the time level t^n. The symbol Δt represents the time step increment, i.e., $\Delta t = t^{n+1} - t^n$. Equation (5) is part of the predictor stage of a two-stage time integration scheme, which provides an intermediate estimate $\overline{u}_i^{n+1}$ of the solution at the next time level. Here, u_i^n denotes the numerical approximation to the exact solution $u(x_i, t^n)$, where $x_i = i\Delta x$ and $t^n = n\Delta t$are the discrete spatial and temporal grid points, respectively. The derivative $\left.\frac{\partial u}{\partial t}\right|_i^n$ represents the temporal derivative of u at point (x_i, t^n).

Step 2: Corrector Stage:

The second stage corrects the predicted value:

$$u_i^{n+1} = au_i^n + b\overline{u}_i^{n+1} + c\left(e^{\Delta t} - 1\right)\left\{\left.\frac{\partial \overline{u}}{\partial t}\right|_i^{n+1}\right\} \tag{6}$$

Where a, b, and c are unknown, which will be found by matching the Taylor series Expansion of terms on both sides of the scheme.

The Taylor series Expansion for u_i^{n+1} is expressed as

$$u_i^{n+1} = u_i^n + \Delta t\left.\frac{\partial u}{\partial t}\right|_i^n + \frac{(\Delta t)^2}{2}\left.\frac{\partial^2 u}{\partial t^2}\right|_i^n + O\left((\Delta t)^3\right) \tag{7}$$

Now, substituting Eqs. (5) and (7) into Eq. (6) as

$$\begin{aligned} u_i^n + \Delta t\left.\frac{\partial u}{\partial t}\right|_i^n + \frac{(\Delta t)^2}{2}\left.\frac{\partial^2 u}{\partial t^2}\right|_i^n = au_i^n + b\Bigg(&\frac{1}{2}u_i^n e^{5\Delta t} + \frac{1}{2}u_i^n e^{-4\Delta t} \\ &+ \left(e^{5\Delta t} + e^{-4\Delta t} - 2\right)\left\{\left.\frac{\partial u}{\partial t}\right|_i^n - \frac{1}{2}u_i^n\right\}\Bigg) \\ &+ c\left(e^{\Delta t} - 1\right)\Bigg\{\frac{1}{2}e^{5\Delta t}\left.\frac{\partial u}{\partial t}\right|_i^n + \frac{1}{2}e^{-4\Delta t}\left.\frac{\partial u}{\partial t}\right|_i^n \\ &+ \left(e^{5\Delta t} + e^{-4\Delta t} - 2\right)\left(\left.\frac{\partial^2 u}{\partial t^2}\right|_i^n - \frac{1}{2}\left.\frac{\partial u}{\partial t}\right|_i^n\right)\Bigg\} \end{aligned} \tag{8}$$

Now equating u_i^n, $\left.\frac{\partial u}{\partial t}\right|_i^n$ and $\left.\frac{\partial^2 u}{\partial t^2}\right|_i^n$ on both sides of Eq. (8), it yields

$$\left.\begin{aligned} 1 &= a + \tfrac{b}{2}\left(e^{5\Delta t} + e^{-4\Delta t}\right) - \tfrac{b}{2}\left(e^{5\Delta t} + e^{-4\Delta t} - 2\right) \\ \Delta t &= b\left(e^{5\Delta t} + e^{-4\Delta t} - 2\right) + c\left(e^{\Delta t} - 1\right)\left\{\tfrac{1}{2}e^{5\Delta t} + \tfrac{1}{2}e^{-4\Delta t} - \tfrac{1}{2}\left(e^{5\Delta t} + e^{-4\Delta t} - 2\right)\right\} \\ \tfrac{(\Delta t)^2}{2} &= c\left(e^{\Delta t} - 1\right)\left(e^{5\Delta t} + e^{-4\Delta t} - 2\right) \end{aligned}\right\} \tag{9}$$

By solving the system of Eqs. (9), the values of a, b, and c can be determined as follows. To do this, we consider a specific and commonly used value of the time step Δt in the stability region of the scheme, say $\Delta t = 0.1$. Substituting this into the system of equations (9), we solve numerically:

$$\left.\begin{aligned} 1 &= a + \tfrac{b}{2}\left(e^{0.5} + e^{-0.4}\right) - \tfrac{b}{2}\left(e^{0.5} + e^{-0.4} - 2\right) \\ 0.1 &= b\left(e^{0.5} + e^{-0.4} - 2\right) + c\left(e^{0.1} - 1\right)\left\{\tfrac{1}{2}e^{0.5} + \tfrac{1}{2}e^{-0.4} - \tfrac{1}{2}\left(e^{0.5} + e^{-0.4} - 2\right)\right\} \\ \tfrac{(0.1)^2}{2} &= c\left(e^{0.1} - 1\right)\left(e^{0.5} + e^{-0.4} - 2\right) \end{aligned}\right\}$$

Solving this, we obtain $a = 0.4291$, $b = 0.5082$, and $c = 0.062$. These values ensure that the scheme matches the Taylor Expansion of the exact solution up to the second order and maintains the intended temporal accuracy. This system ensures second-order temporal accuracy.

The proposed scheme for the first component of deterministic fuzzy Eq. (3) is expressed as

$$\overline{(\overleftrightarrow{u})}_i^{n+1} = \frac{1}{2}(\overleftrightarrow{u}_1)_i^n e^{5\Delta t} + \frac{1}{2}(\overleftrightarrow{u}_1)_i^n e^{-4\Delta t} + \left(e^{5\Delta t} + e^{-4\Delta t} - 2\right)\left\{0.4\beta_1 \frac{\partial^2 \overleftrightarrow{u}_1}{\partial x^2}\bigg|_i^n + f(\overleftrightarrow{u})_i^n - \frac{1}{2}(\overleftrightarrow{u}_1)_i^n\right\} \tag{10}$$

$$\left(\overleftrightarrow{u}_1\right)_i^{n+1} = a\left(\overleftrightarrow{u}_1\right)_i^n + b\overline{\left(\overleftrightarrow{u}\right)}_i^{n+1} + c\left(e^{\Delta t} - 1\right)\{0.4\beta_1 \frac{\partial^2}{\partial x^2}\overline{\left(\overleftrightarrow{u}\right)}_i^{n+1} + f\overline{\left(\overleftrightarrow{u}\right)}_i^{n+1}\} \tag{11}$$

For simplicity, the component $\left(\overleftrightarrow{u}_1\right)_i^1$ is expressed as u_i^n.

3.2 *Space discretization*

The compact scheme is used for space discretization of Eq. (3). The compact scheme is expressed as

$$\overline{u}_i^{n+1} = \frac{1}{2}u_i^n e^{5\Delta t} + \frac{1}{2}u_i^n e^{-4\Delta t} + \left(e^{5\Delta t} + e^{-4\Delta t} - 2\right)\left\{0.4\beta_1 C^{-1} D u_i^n + f u_i^n - \frac{1}{2}u_i^n\right\} \tag{12}$$

$$u_i^{n+1} = a u_i^n + b\overline{u}_i^{n+1} + c\left(e^{\Delta t} - 1\right)\{0.4\beta_1 C^{-1} D\overline{u}_i^{n+1} + f\overline{u}_i^{n+1}\} \tag{13}$$

Where C and D are matrices containing the left and right sides of the following equations. We adopt a sixth-order three-point compact finite difference scheme for approximating the second-order derivative $\frac{\partial^2 u}{\partial x^2}$. The general form of the scheme is:

$$\gamma_1\, u''\big|_{i-1}^n + u''\big|_i^n + \gamma_1\, u''\big|_{i+1}^n = c_\circ \frac{(u_{i+1}^n - 2u_i^n + u_{i-1}^n)}{(\Delta x)^2} + c_1 \frac{(u_{i+2}^n - 2u_i^n + u_{i-2}^n)}{4(\Delta x)^2} \tag{14}$$

Where γ_1 is a free parameter and $c_\circ$ and c_1 are expressed as

$$c_\circ = \frac{4}{3}(1-\gamma_1),\, c_1 = \frac{1}{3}(10\gamma_1 - 1).$$

This leads to a linear system of the form $C\mathbf{U}^{''} = D\mathbf{U}$.

Where $\mathbf{U}$ is a vector of unknowns $[u_1, u_2, \ldots, u_{N-1}]^T$, C is a tridiagonal matrix representing the left-hand side coefficients, D is a banded matrix capturing the discrete spatial operator on the right-hand side.

3.3 *Explicit form of matrices C and D*

Matrix C is defined as:

$$C = \begin{bmatrix} 1 & \gamma_1 & 0 & \cdots & 0 \\ \gamma_1 & 1 & \gamma_1 & \cdots & 0 \\ 0 & \gamma_1 & 1 & \ddots & \vdots \\ \vdots & \ddots & \ddots & \ddots & \gamma_1 \\ 0 & \ldots & 0 & \gamma_1 & 1 \end{bmatrix}$$

Matrix D is defined as: Matrix D is constructed to approximate the right-hand side of the following discretization: $\gamma_1\, u''|_{i-1}^n + u''|_i^n + \gamma_1\, u''|_{i+1}^n = c_\circ \frac{(u_{i+1}^n - 2u_i^n + u_{i-1}^n)}{(\Delta x)^2} + c_1 \frac{(u_{i+2}^n - 2u_i^n + u_{i-2}^n)}{4(\Delta x)^2}$. The full spatial discretization matrix $D\varepsilon R^{(N-1)\times(N-1)}$ is written as: $D = \frac{1}{(\Delta x)\hat{}2}\left[c_o \cdot T_3 + \frac{c_1}{4} \cdot T_5\right]$ where T_3 is a classical tridiagonal matrix and is defined as below:

$$T_3 = \begin{bmatrix} -2 & 1 & 0 & \cdots & 0 \\ 1 & -2 & 1 & \cdots & 0 \\ 0 & 1 & -2 & \ddots & \vdots \\ \vdots & \ddots & \ddots & \ddots & 1 \\ 0 & \ldots & 0 & 1 & -2 \end{bmatrix}$$

Also, the T_5 five-point band matrix (second off-diagonals) is defined as

$$T_5 = \begin{bmatrix} -2 & 0 & 1 & 0 & \cdots & 0 \\ 0 & -2 & 0 & 1 & \cdots & 0 \\ 1 & 0 & -2 & 0 & \ldots & 0 \\ 0 & 1 & 0 & -2 & \ldots & 0 \\ \vdots & \ddots & \ddots & \ddots & \ddots & 1 \\ 0 & \ldots & 0 & 1 & 0 & -2 \end{bmatrix}$$

3.4 *Incorporating stochasticity*

Now, the fuzzy stochastic equation is expressed as

$$\partial u = 0.4\beta_1 \frac{\partial^2 u}{\partial x^2} dt + f(u)dt + \sigma_1 u dW \tag{15}$$

Where W in Eq. (15) is the Wiener process. For the stochastic term $\sigma_1 udW$ approximate the Wiener increment ΔW as a normally distributed random variable with mean 0 and variance Δt : $\Delta W \sim N(0, \Delta t)$.

The first stage of the scheme for Eq. (15) is the same as Eq. (12), while the second stage is expressed as

$$u_i^{n+1} = au_i^n + b\overline{u}_i^{n+1} + c\left(e^{\Delta t} - 1\right)\left\{0.4\beta_1 C^{-1} D\overline{u}_i^{n+1} + f\overline{u}_i^{n+1}\right\} + \sigma u_i^n \Delta W \tag{16}$$

Where $\Delta W \sim (W^{n+1} - W^n)$ is approximated by a normal distribution $N(0, \Delta t)$, and C, D are matrices representing the compact scheme coefficients.

This two-stage predictor-corrector scheme effectively addresses the challenges posed by nonlinearity, randomness, and fuzziness in Stochastic Partial Differential Equations (SPDEs), providing a robust computational approach for such complex systems. The proposed two-stage method, combined with the sixth-order compact discretization in space, yields an overall explicit scheme, since all updates at time level $n + 1$ are computed from known quantities at time level n and do not require solving non-linear algebraic systems.

3.5 *Key differences introduced by the fuzzy parameter α_1*

The fuzzy parameter α_1, modelled as a triangular fuzzy number, is handled through the β_1-cut approach, which transforms the fuzzy Partial Differential Equations (PDE) into a family of interval-valued problems for each $\beta_1 \in [0, 1]$. This leads to two bounding solutions $u_1(t, x, \beta_1)$ and $u_2(t, x, \beta_1)$, rather than a single crisp solution. While the numerical stencil structure remains the same, the input parameters and computed solution are interval-valued functions, requiring the numerical method to be applied twice (for lower and upper bounds) or in a parametric form. This introduces uncertainty quantification directly into the numerical solution process, which is unnecessary for classical PDEs. In classical PDEs, numerical methods produce a single trajectory. In fuzzy PDEs, the output is a fuzzy-valued function interpreted via its membership function or its β_1-Cut bounds are essential for applications where uncertainty is present in parameters.

4. Stability analysis

To determine the conditions under which differential equations are stable, one might utilize the Fourier series analysis, often known as the Von Neumann stability analysis. This analysis provides exact conditions for linear partial differential equations; for non-linear differential equations, it estimates the stability condition. This analysis is based on transformations that reduce differences into trigonometric equations. To apply this analysis, consider the transformations

$$Ce^{iI\phi} = \gamma_1 e^{(i-1)I\phi} + e^{iI\phi} + \gamma_1 e^{(i+1)I\phi} \tag{17}$$

$$De^{iI\phi} = c_\circ \frac{(e^{(i-1)I\phi} - 2e^{iI\phi} + e^{(i+1)I\phi})}{(\Delta x)^2} + c_1 \frac{(e^{(i-2)I\phi} - 2e^{iI\phi} + e^{(i+2)I\phi})}{4(\Delta x)^2} \tag{18}$$

By substituting Eqs. (17) and (18) into the first stage of the scheme (12) with $f = 0$ it is obtained

$$\overline{u}_i^{n+1} = \frac{1}{2}u_i^n e^{5\Delta t} + \frac{1}{2}u_i^n e^{-4\Delta t} + \left(e^{5\Delta t} + e^{-4\Delta t} - 2\right)\left\{0.4\beta_1\left(\frac{4c_\circ(\cos\phi - 1) + c_1(cos2\phi - 1)}{2(\Delta x)^2(2\gamma_1\cos\phi + 1)}\right) - \frac{1}{2}\right\}u_i^n \tag{19}$$

Write Eq. (19) as

$$\overline{u}_i^{n+1} = \alpha u_i^n \tag{20}$$

Where $\alpha = \frac{1}{2}e^{5\Delta t} + \frac{1}{2}e^{-4\Delta t} + \left(e^{5\Delta t} + e^{-4\Delta t} - 2\right)\left\{0.4\beta_1\left(\frac{4c_\circ(\cos\phi-1)+c_1(cos2\phi-1)}{2(\Delta x)^2(2\gamma_1\cos\phi+1)}\right) - \frac{1}{2}\right\}$.
Now substituting transformations (17), (18), and Eq. (20) into the second stage (16) with $f = 0$ as

$$u_i^{n+1} = au_i^n + b\alpha u_i^n + c\left(e^{\Delta t} - 1\right)\left\{0.4\beta_1\left(\frac{4c_\circ(\cos\phi - 1) + c_1(cos2\phi - 1)}{2(\Delta x)^2(2\gamma_1\cos\phi + 1)}\right)\right\}\alpha u_i^n + \sigma u_i^n \Delta W \tag{21}$$

Rewrite Eq. (21) as

$$u_i^{n+1} = \alpha_1 u_i^n + \sigma u_i^n \Delta W \tag{22}$$

The amplification factor is given as

$$\frac{u_i^{n+1}}{u_i^n} = \alpha_1 + \sigma\Delta W \tag{23}$$

By applying the expected value on the square of the amplification factor as

$$E\left|\frac{u_i^{n+1}}{u_i^n}\right|^2 = 2E\left|\alpha_1\right|^2 + 2\sigma^2 E|\Delta W|^2 = \lceil\alpha_1\rceil^2 + \sigma^2\Delta t \tag{24}$$

If $|\alpha_1|^2 < \frac{1}{2}$ and assume that $2\sigma^2 = \lambda$, then inequality (24) is expressed as

$$E\left|\frac{u_i^{n+1}}{u_i^n}\right|^2 \leq 1 + \lambda\Delta t \tag{25}$$

From the above inequality and the derived conditions, we conclude the following: The scheme exhibits stability in the mean square sense, provided that $\lceil\alpha_1\rceil^2 < 1$. However, since α_1 depends on Δt, Δx, and other parameters (see Eq. (22)), the stability is conditional and governed by both time and spatial steps, specifically the mesh ratio $\frac{\Delta t}{\Delta x^2}$.

Mesh Ratio Restriction: From Equation (20), we observe that α and hence α_1 grows with Δt and $\frac{1}{\Delta x^2}$. Therefore, to maintain $\lceil\alpha_1\rceil^2 < 1$, the following equation must be imposed $\frac{\Delta t}{\Delta x^2} \leq C$, for some constant $C > 0$. Hence, the scheme is conditionally stable, and the mesh ratio is restricted.

Theorem 1 The proposed time and compact scheme in space Eq. (12) and Eq. (16) is consistent in the mean square sense.

Proof. Let F be a smooth function, then

$$L(F)_i^n = F\left((n+1)\Delta t, i\Delta x\right) - F(n\Delta t, i\Delta x) - 0.4\beta_1\int_{n\Delta t}^{(n+1)\Delta t} F_{xx}(s, i\Delta x)dS - \sigma\int_{n\Delta t}^{(n+1)\Delta t} F(s, i\Delta x)dW(s) \tag{26}$$

Where $L(F_i^n)$ is the exact operator applied to the test function F.

$$\begin{aligned} L_i^n F =& F\left((n+1)\Delta t,\, i\Delta x\right) - F(n\Delta t,\, i\Delta x) - 0.4\beta_1 b\left(e^{5\Delta t} + e^{-4\Delta t} - 2\right) C^{-1} DF(n\Delta t,\, i\Delta x) \\ & - c0.4\beta_1\left(e^{\Delta t} - 1\right) C^{-1} D\overline{F}\left((n+1)\Delta t,\, i\Delta x\right) - \sigma F(n\Delta t,\, i\Delta x)\left(W\left((n+1)\Delta t\right) - W(n\Delta t)\right) \end{aligned} \tag{27}$$

Where $L_i^n F$ is the numerical operator obtained from the proposed scheme.

Where $\overline{F}\left((n+1)\Delta t,\, i\Delta x\right) = \frac{1}{2}F\left((n+1)\Delta t,\, i\Delta x\right)e^{5\Delta t} + \frac{1}{2}F(n\Delta t,\, i\Delta x)e^{-4\Delta t} + \left(e^{5\Delta t} + e^{-4\Delta t} - 2\right)\left\{C^{-1}DF(n\Delta t,\, i\Delta x)\right.$ $\left. - \frac{1}{2}F(n\Delta t,\, i\Delta x)\right.$.

The following equation can be obtained from Eq. (26) and Eq. (27)

$$\begin{aligned} E\left|L(F)_i^n - L_i^n F\right|^2 \le E\Bigg| & - 0.4\beta_1 \int_{n\Delta t}^{(n+1)\Delta t} F_{xx}(s,\, i\Delta x)\, dS - \sigma \int_{n\Delta t}^{(n+1)\Delta t} F(s,\, i\Delta x)\, dW(s) \\ & + b\left(e^{5\Delta t} + e^{-4\Delta t} - 2\right) 0.4\beta C^{-1} DF(n\Delta t,\, i\Delta x) \\ & - 0.4\beta_1\left(e^{\Delta t} - 1\right) C^{-1} D\overline{F}\left((n+1)\Delta t,\, i\Delta x\right) \\ & + \sigma F(n\Delta t,\, i\Delta x)\left(W\left((n+1)\Delta t\right) - W(n\Delta t)\right)\Bigg|^2 \end{aligned} \tag{28}$$

Eq. (28) implies

$$\begin{aligned} E\left|L(F)_i^n - L_i^n F\right|^2 \le 2\left(0.4\beta_1\right)^2 E\Bigg| & \int_{n\Delta t}^{(n+1)\Delta t} F_{xx}(s,\, i\Delta x)\, dS - b\left(e^{5\Delta t} + e^{-4\Delta t} - 2\right) C^{-1} DF(n\Delta t,\, i\Delta x) \\ & + c\left(e^{\Delta t} - 1\right) C^{-1} D\overline{F}\left((n+1)\Delta t,\, i\Delta x\right)\Bigg|^2 \\ & + 2\sigma^2 E\Bigg| \int_{n\Delta t}^{(n+1)\Delta t} F(s,\, i\Delta x)\, dW(s) \\ & - F(n\Delta t,\, i\Delta x)\left(W\left((n+1)\Delta t\right) - W(n\Delta t)\right)\Bigg|^2 \end{aligned} \tag{29}$$

Now using the inequality

$$E\left|\int_{t_\circ}^{t} v(s,\, w) dw(s)\right|^{2m} \le (t - t_\circ)^{m-1}\left[m(2m-1)\right]^m \int_{t_\circ}^{t} E\left[\left|v(s,\, w)\right|^{2m}\right] ds \tag{30}$$

inequality (29), it yields

$$
\begin{aligned}
E\left|L(F)_i^n - L_i^n F\right|^2 \leq 2\left(0.4\beta_1\right)^2 E\Bigg| & \int_{n\Delta t}^{(n+1)\Delta t} F_{xx}(s, i\Delta x)\, dS \\
& - b\left(e^{5\Delta t} + e^{-4\Delta t} - 2\right) C^{-1} DF(n\Delta t, i\Delta x) \\
& + c\left(e^{\Delta t} - 1\right) C^{-1} D\overline{F}\left((n+1)\Delta t, i\Delta x\right)\Bigg|^2 \\
& + 2\sigma^2 \Delta t \int_{n\Delta t}^{(n+1)\Delta t} \left[\left|F(s, i\Delta x) - F(n\Delta t, i\Delta x)\left(W\left((n+1)\Delta t\right) - W(n\Delta t)\right)\right|^2\right]
\end{aligned} \tag{31}
$$

Now, applying the *limit* as $\Delta x \to 0$, $\Delta t \to 0$, $t = (n+1)\Delta t$, $(n\Delta t, i\Delta x) \to (t, x)$, then the mean square error tends to zero. i.e.

$$
E\left|L\left(F_i^n\right) - L_i^n F\right|^2 \to 0 \tag{32}
$$

The scheme is consistent in the mean square sense if: $\lim_{\Delta t \to 0,\, \Delta x \to 0} E[|L(F_i^n) - L_i^n F|^2] = 0$. This condition is derived from the error expression (Equation (31)), which involves temporal discretization error, controlled by Taylor expansions and exponential integrators; spatial discretization error, controlled by the sixth-order compact scheme; and stochastic integral approximation error, controlled by Itô isometry and standard inequalities. The inequality (31) is now rewritten to highlight that all error terms vanish in the limit:

$$
E\left|L\left(F_i^n\right) - L_i^n F\right|^2 \leq C_1 \Delta t^2 + C_2 \Delta x^4 + C_3 \Delta t \to 0 \text{ as } \Delta t, \Delta x \to 0
$$

This verifies that the local truncation error converges to zero in the mean-square sense, indicating that the method is consistent with the original stochastic partial differential equation. Consequently, the suggested approach for temporal and compact discretization is consistent in the mean-square sense.

4.1 *Convergence of the fully discrete scheme*

Let $u(x, t)$ be the exact solution of the fuzzy stochastic partial differential equation and let u_i^n be the fully discrete approximation obtained from the proposed two-stage compact scheme. Then, under suitable regularity assumptions on the solution and boundedness of the noise coefficients, the numerical scheme satisfies the convergence estimate:

$$
\lim_{\Delta t \to 0,\, \Delta x \to 0} E[|u(x_i, t^n) - u_i^n|^2] = 0
$$

This ensures that the scheme converges to the true solution in the mean-square norm as the mesh is refined. Due to the presence of both stochastic and fuzzy components, an exact convergence rate is not derived in this work. However, numerical simulations (Figures 1-8) validate the proposed scheme's empirical convergence and superior performance compared to existing methods.

5. Mathematical model

The SIR model is a foundational framework in epidemiology. A SIR model is simple yet powerful. The model consists of susceptible, infective, and recovered people. The symbol S is used for susceptible (Individuals who can contract the disease), I (Individuals currently carrying and capable of transmitting the disease) is for infective, and R (Individuals who have recovered from the disease and are no longer susceptible) for recovered people. The SIR model is extended by considering β, the interaction rate, to be a variable quantity. To enhance the model's realism, especially for diseases with time-varying transmission rates, the transmission rate β is treated as a dynamic variable influenced by factors such as behavioural changes and interventions. Incorporating spatial considerations, the SIR model can be extended to account for the diffusion of individuals across regions, leading to the following system of partial differential equations:

$$\frac{\partial S}{\partial t} = d_1 \frac{\partial^2 S}{\partial x^2} + \Lambda - \beta SI - (\mu + \delta)S \tag{33}$$

$$\frac{\partial I}{\partial t} = d_2 \frac{\partial^2 I}{\partial x^2} + \beta SI - (\mu + \theta + \gamma)I \tag{34}$$

$$\frac{\partial R}{\partial t} = d_3 \frac{\partial^2 R}{\partial x^2} + \gamma I + \delta S - \mu R \tag{35}$$

$$\frac{\partial \beta}{\partial t} = d_4 \frac{\partial^2 \beta}{\partial x^2} + \frac{\beta_2}{1 + c_1 I} - \alpha\beta \tag{36}$$

Where d_1, d_2, d_3, d_4 are diffusion coefficients for the susceptible, infective, recovered populations, and the transmission rate, respectively, representing the spatial spread due to movement, Λ is birth rate introducing new susceptible individuals into the population, μ is natural death rate accounting for the regular mortality unrelated to the disease, θ is molarity rate of the disease, representing the fatality among the infected, δ denotes effect immunization rate of the susceptible population following vaccination, moving them directly to the recovered class, γ represents the rate at which the infected people recovered, transitioning them to the recovered class. β_2 denotes the maximum potential transmission rate in the absence of infective individuals, $c_1$is the coefficient modulating the impact of the infective population on reducing the transmission rate, possibly due to saturation effects or behavioural changes, and α represents the decay rate of the transmission rate, reflecting the natural decline of β over time in the absence of new infections.

5.1 *Modelling dynamics*

Susceptible Population S: This group increases through births Λ and decreases due to natural deaths μS, disease-induced immunization δS, and new infections βSI. The diffusion term $d_1\nabla^2 S$ captures the spatial movement of susceptible individuals.

Infective Population I: Infections occur at a rate proportional to both susceptible and infective individuals βSI. The infective population decreases due to natural deaths μI, disease-induced deaths θI, recoveries γI, and spatial movement $d_2\nabla^2 I$.

Recovered Population R: Individuals enter this compartment through recovery γI and immunization δS. Losses occur due to natural deaths μR and spatial movement $d_3\nabla^2 R$.

Transmission Rate β: The evolution of β is influenced by its diffusion $d_4\nabla^2\beta$, a source term representing the maximum transmission rate modulated by the infective population $\frac{\beta_2}{1+c_1 I}$, and a decay term $\alpha\beta$, indicating the natural reduction of transmission potential over time.

For the system of Eqs. (33)-(36) with $d_1 = d_2 = d_3 = d_4 = 0$, the following equations

$$\left.\begin{aligned} &\Lambda-\beta \mathrm{SI}-(\mu+\delta)\mathrm{S}=0 \\ &\beta \mathrm{SI}-(\mu+\theta+\gamma)\mathrm{I}=0 \\ &\gamma \mathrm{I}+\delta \mathrm{S}-\mu \mathrm{R}=0 \\ &\frac{\beta_2}{1+c_1 I}-\alpha\beta=0 \end{aligned}\right\} \tag{37}$$

has one of the equilibrium points

$$B^*\left(\frac{\Lambda}{\delta+\mu}, 0, \frac{\delta\Lambda}{\mu(\delta+\mu)}, \frac{\beta_2}{\alpha}\right) \tag{38}$$

Theorem 2 The system of Eqs. (33)-(36) with $d_1=d_2=d_3=d_4=0$ is locally stable.
Proof. The Jacobian of Eq. (33)-(36) using $d_1=d_2=d_3=d_4=0$ can be written as

$$J=\begin{bmatrix} -\delta-\beta I-\mu & \beta S & 0 & -IS \\ \beta I & -\gamma-\mu+\beta S-\theta & 0 & IS \\ S & \gamma & -\mu & 0 \\ 0 & -\frac{\beta_2 c_1}{(1+c_1 I)^2} & 0 & -\alpha \end{bmatrix} \tag{39}$$

The Jacobian at the equilibrium point B^* is given as

$$J|_{B^*}=\begin{bmatrix} -\delta-\mu & \frac{\beta_2\Lambda}{\alpha(\delta+\mu)} & 0 & 0 \\ 0 & -\gamma-\mu+\frac{\beta_2\Lambda}{\alpha(\delta+\mu)}-\theta & 0 & 0 \\ \delta & \gamma & -\mu & 0 \\ 0 & -\beta_2 c_1 & 0 & -\alpha \end{bmatrix} \tag{40}$$

The eigenvalue for $J|_{B^*}$ are expressed as

$$\lambda_1=-\alpha,\ \lambda_2=-\mu,\ \lambda_3=-\delta-\mu,\ \lambda_4=\frac{1}{\alpha(\delta+\mu)}\left[-\alpha\delta\gamma-\alpha\delta\mu-\alpha\gamma\mu-\alpha\mu^2+\beta_2\Lambda-\alpha\delta\theta-\alpha\mu\theta\right]$$

Now λ_4 will be negative if

$$\beta_2\Lambda < \alpha\delta\gamma + \alpha\delta\mu + \alpha\gamma\mu + \alpha\mu^2 + \alpha\delta\theta + \alpha\mu\theta.$$

5.2 *Incorporating fuzziness and stochasticity*

These parameters can be modelled as triangular fuzzy numbers to address uncertainties in the natural death rate u and the immunization rate δ, which may not be precisely known or may vary. This approach acknowledges the inherent variability and imprecision in real-world data. Additionally, to capture random fluctuations and external shocks, Fuzzy Stochastic Differential Equations (FSDEs) are introduced:

$$dS = \left(d_1\frac{\partial^2 S}{\partial x^2} + \Lambda - \beta SI - (\mu+\delta)S\right)dt + \sigma_1 S dW \tag{41}$$

$$dI = (d_2\frac{\partial^2 I}{\partial x^2} + \beta SI - (\mu+\theta+\gamma)I)dt + \sigma_2 I dW \tag{42}$$

$$dR = (d_3\frac{\partial^2 R}{\partial x^2} + \gamma I + \delta S - \mu R)dt + \sigma_3 R dW \tag{43}$$

$$d\beta = \left(d_4\frac{\partial^2 \beta}{\partial x^2} + \frac{\beta_2}{1+c_1 I} - \alpha\beta\right)dt + \sigma_4\beta dW \tag{44}$$

Where μ and δ are triangular fuzzy numbers and σ_1, σ_2, σ_3 and σ_4 represent the intensities of the stochastic perturbations for each compartment, and dW are Wiener processes modelling the random fluctuations. This stochastic framework allows the model to account for unpredictable events and inherent randomness in disease transmission and recovery processes.

By integrating diffusion processes, variable transmission rates, fuzzy parameters, and stochastic elements, this extended SIR model provides a comprehensive framework to for simulating and analyzing the complex dynamics of infectious diseases.

5.2.1 *NSFD scheme for the fuzzy stochastic SIR-β model*

To numerically solve the fuzzy stochastic reaction-diffusion system (41)-(44), we construct a Non-Standard Finite Difference (NSFD) scheme that satisfies the following key features: Positivity and boundedness of the solution, Accurate handling of fuzzy parameters via β-cut formulation, and incorporation of stochastic terms with appropriate discrete approximations.

We first discretize the domain $(x,t)\varepsilon[0,L]\times[0,T]$ using spatial step size Δx and time step Δt, denoting:
$S_i^n \approx S(x_i,t_n)$, I_i^n, R_i^n and β_i^n similarly,

$$x_i = i\Delta x,\ t_n = n\Delta t$$

$\Delta W^n \sim N(0,\Delta t)$ represents the Wiener increment.
The discretized NSFD scheme is then written as follows:

$$\frac{S_i^{n+1}-S_i^n}{\phi(\Delta t)} = d_1\delta_x^2 S_i^n + \Lambda - \beta_i^n S_i^n I_i^n - (\mu+\delta)S_i^n + \sigma_1 S_i^n \Delta W^n \tag{45}$$

$$\frac{I_i^{n+1}-I_i^n}{\phi(\Delta t)} = d_2\delta_x^2 I_i^n + \beta_i^n S_i^n I_i^n - (\mu+\theta+\gamma)I_i^n + +\sigma_2 I_i^n \Delta W^n \tag{46}$$

$$\frac{R_i^{n+1}-R_i^n}{\phi(\Delta t)} = d_3\delta_x^2 R_i^n + \gamma I_i^n + \delta S_i^n - \mu R_i^n + \sigma_3 R_i^n \Delta W^n \tag{47}$$

$$\frac{\beta_i^{n+1}-\beta_i^n}{\phi(\Delta t)} = d_4\delta_x^2 \beta_i^n + \frac{\beta_2}{1+c_1 I_i^n} - \alpha\beta_i^n + \sigma_4\beta\Delta W^n \tag{48}$$

Here $\phi(\Delta t)$ is a non-linear denominator function to improve the dynamic consistency and numerical stability. A typical choice is: $\phi(\Delta t) = \frac{\Delta t}{1-\Delta t}$ and $\delta_x^2 u_i^n$: is the standard second-order central difference: $\delta_x^2 u_i^n = \frac{u_{i+1}^n - 2u_i^n + u_{i-1}^n}{(\Delta x)^2}$. Fuzzy parameters such as μ and δ are evaluated via β-cut representation, where triangular fuzzy numbers are approximated over the interval $[\mu_L, \mu_U]$ with $\beta\varepsilon[0, 1]$, leading to a family of crisp sub-models solved independently and aggregated at the end.

Subject to the boundary conditions: The NSFD scheme supports: Neumann boundary conditions (zero-flux):

$$\frac{\partial u}{\partial x}(0, t) = \frac{\partial u}{\partial x}(L, t) = 0 \tag{49}$$

Which can be discritized as $u_{-1}^n = u_1^n$, $u_{N+1}^n = u_{N-1}^n$.

The scheme maintains positivity for all state variables provided the step sizes satisfy mild constraints. The inclusion of stochastic terms via $\sigma_k u_i^n \Delta W^n$ ensures that randomness is reflected correctly at each step. An NSFD formulation is explicitly used for performance comparison with the proposed scheme (see Section 6).

5.3 *Justification for model complexity (fuzzy + stochastic + β-incidence)*

Fuzziness captures epistemic uncertainty that arises due to imprecise or incomplete knowledge in epidemic parameters, especially during early stages of an outbreak or in regions with inconsistent data reporting. For example, infection rates, recovery rates, and contact behaviour are rarely known precisely. Representing these as triangular fuzzy numbers allows the model to incorporate a realistic range of uncertainty rather than relying on fixed deterministic values.

Stochasticity reflects random fluctuations in disease transmission and recovery processes due to inherent biological randomness and environmental variability. This is especially relevant in localized outbreaks or small populations, where chance events significantly influence disease progression. The incorporation of a Wiener process in our model introduces this necessary randomness into the simulation.

The non-linear β-incidence function reflects saturation effects and behavioural responses in the transmission dynamics, which cannot be captured by classical bilinear incidence terms. For instance, as infection spreads, public awareness and healthcare limitations affect how contacts lead to new infections β-incidence better models this adaptive behaviour.

6. Results and discussions

We present a detailed simulation study with the following objectives:

1. An explicit two-stage numerical scheme is proposed for solving both deterministic and stochastic partial differential equations.

2. The scheme is constructed on two levels, making it self-contained and not dependent on other solvers.

3. It is conditionally stable in the mean square sense, implying: Restrictions on allowable time and space step sizes. Careful selection of model parameters is necessary to ensure numerical stability.

4. The first stage of the scheme ignores the stochastic (Wiener process) term. It is identical for both deterministic and stochastic equations. The second stage incorporates the stochastic component of the PDE. Behaves similarly to the Euler-Maruyama method, a standard method for SDEs.

5. The proposed scheme achieves second-order accuracy in time for deterministic problems. In contrast, the traditional Euler-Maruyama method is only first-order accurate for such problems.

6.1 *Comparison between the two numerical methods*

To solve the stochastic fuzzy SIR-β model, Figure 1 compares the suggested two-stage numerical methodology with the Euler-Maruyama method. The Figure consists of two plots displaying the evolution of the Susceptible S, Infective I, Recovered R populations and the transmission rate $\beta(t)$ over time under identical parameter settings: $d_1 = d_2 = d_3 = d_4 = 0.1$, $\mu = 0.1$, $\alpha = 0.3$, $\gamma = 0.1$, $c_1 = 0.1$, $\Lambda = 0.1$, $\delta = 0.1$, $\beta_1 = 0.1$, $\theta = 0.1$. The number of susceptible individuals $S(t)$ decreases over time as people either become infected or gain immunity through vaccination δ. The rate of decline is similar in both plots, confirming that both numerical schemes capture the dynamics consistently. The number of infective individuals $I(t)$ initially rises before declining sharply. The decline is driven by recovery γI, deaths θI, and a reduction in available susceptible individuals. The stochastic fluctuations are visible in the right plot, corresponding to the Euler-Maruyama method. The recovered population $R(t)$ increases as infected individuals recover or get immunized. The red curves in both plots show a steady increase, with slight variations due to stochastic effects. The infection transmission rate $\beta(t)$ decreases over time, governed by the equation $\frac{\partial \beta}{\partial t} = d_4 \frac{\partial^2 \beta}{\partial x^2} + \frac{\beta_2}{1+c_1 I} - \alpha\beta$. As the number of infective individuals decreases, the transmission rate drops due to the dynamic nature of $\beta(t)$. The decay rate is nearly identical in both methods, with the right plot showing slight stochastic variations.

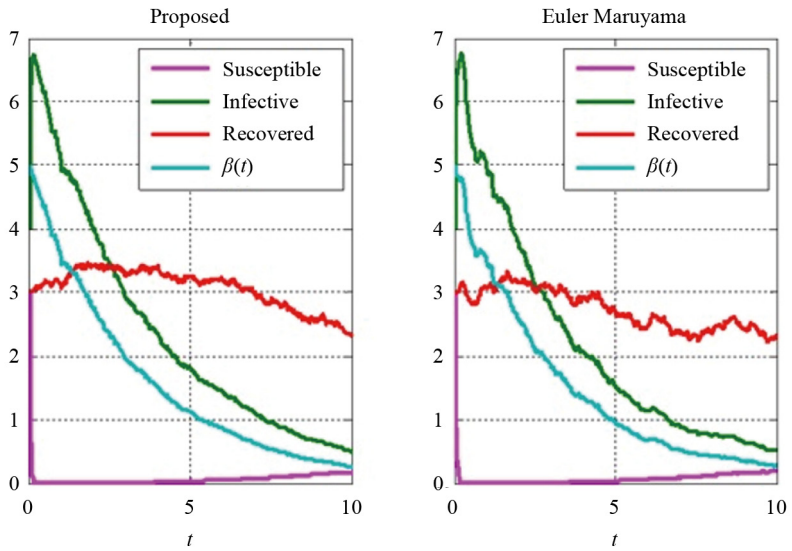

Figure 1. Comparison of proposed and Euler Maruyama method using $d_1 = d_2 = d_3 = d_4 = 0.1$, $\mu = 0.1$, $\alpha = 0.3$, $\gamma = 0.1$, $c_1 = 0.1$, $\Lambda = 0.1$, $\delta = 0.1$, $\beta_1 = 0.1$, $\theta = 0.1$

Solutions derived from the suggested two-stage scheme are shown on the left plot, while those derived from the Euler-Maruyama approach are shown on the right plot. The Euler-Maruyama method introduces visible stochastic fluctuations in the curves, especially for $\beta(t)$ and $I(t)$. The proposed scheme, which is second-order accurate in time, produces smoother curves, indicating better numerical stability and accuracy. Despite the fluctuations, both methods preserve the qualitative dynamics of the system, confirming that the proposed scheme correctly models the stochastic epidemic process. This comparison suggests that the proposed scheme is preferable for accurate long-term predictions, especially in stochastic epidemic models where stability is crucial.

Both panels exhibit fluctuations driven by stochastic effects σ_j, and these are not artefacts of numerical instability. The proposed scheme (left) maintains better stability in the mean-square sense and second-order temporal accuracy, compared to Euler-Maruyama (right), which is first-order accurate.

6.1.1 *Clarifying the purpose of the comparison*

The aim of Figure 1 is not to suggest a visually smoother trajectory, but to compare the accuracy of the proposed scheme with a known first-order stochastic method (Euler-Maruyama), and demonstrate the improved stability in the mean-square sense and higher temporal order of accuracy of the proposed method under identical parameter settings. Both methods are applied to the same stochastic fuzzy SIR-β system, and due to the presence of stochastic noise σ_j, the fluctuations are expected. However, the proposed scheme demonstrates better numerical consistency across realizations due to the refined temporal discretization enabled by the modified exponential integrator and the predictor-corrector approach.

6.1.2 *Clarification on the role of stochasticity in Figures*

The stochastic contribution in the Figures (e.g., Figure 1 and Figures 5-8) can be observed through the deviation and spread in the solution trajectories when the noise term σudW is active. In deterministic cases, trajectories remain smooth, whereas in stochastic cases, the evolution exhibits slight fluctuations that capture the random effects of disease transmission. In contrast to the Euler-Maruyama approach, the suggested scheme preserves numerical stability and provides smoother accuracy in stochastic settings, highlighting this difference.

6.2 *Impact of social behaviour on infection rates (Figure 2)*

Figure 2 illustrates the effect of people's resistance to changing their behaviour on the fuzzy infection rate in a stochastic fuzzy SIR-β model. The curves represent the evolution of the upper β^1 and lower β^2 bounds of the fuzzy infection rate for different values of α, which denotes the decay rate of β. The simulation is performed using the following parameters: $d_1 = d_2 = d_3 = d_4 = 0.1$, $\mu = 0.1$, $\gamma = 0.1$, $c_1 = 0.1$, $\Lambda = 0.1$, $\beta_1 = 0.1$, $\theta = 0.1$. All curves show a monotonic decline in the infection rate $\beta(t)$, indicating that as time progresses, the effective transmission rate decreases. This aligns with real-world scenarios in which public awareness, immune development, and interventions reduce transmission over time. The solid and dashed curves represent β^1 (upper bound of the fuzzy infection rate) for $\alpha = 0.1$ and $\alpha = 0.3$, respectively. The dashed and dotted curves represent β^2 (lower bound of the fuzzy infection rate) for $\alpha = 0.1$ and $\alpha = 0.3$, respectively. As α increases from 0.1 to 0.3, both β^1 and β^2 decrease more rapidly, implying that a higher transmission decay rate reduces the infection rate faster. People's resistance to changing social behaviour (such as refusal to adhere to preventive measures) directly affects the rate at which $\beta(t)$ declines. Higher resistance slows down the decay of $\beta(t)$, keeping the transmission rate higher for longer. In contrast, lower resistance (or better compliance with interventions like social distancing and mask-wearing) leads to a faster decline in $\beta(t)$. When people actively reduce interactions and follow public health guidelines, the infection rate decreases more rapidly $\alpha = 0.3$. If people resist changing their social behaviour, the infection rate remains higher for a longer duration, prolonging the epidemic $\alpha = 0.1$. This Figure highlights the importance of early and effective interventions to reduce disease transmission.

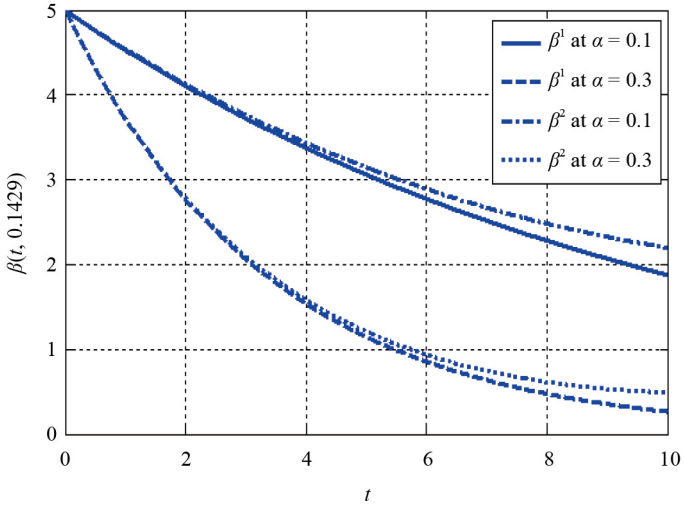

Figure 2. Effect of people resistance to the fuzzy infection rate using $d_1 = d_2 = d_3 = d_4 = 0.1$, $\mu = 0.1$, $\gamma = 0.1$, $c_1 = 0.1$, $\Lambda = 0.1$, $\beta_1 = 0.1$, $\theta = 0.1$

6.3 *Effect of recovery rates on infective and recovered populations (Figure 3)*

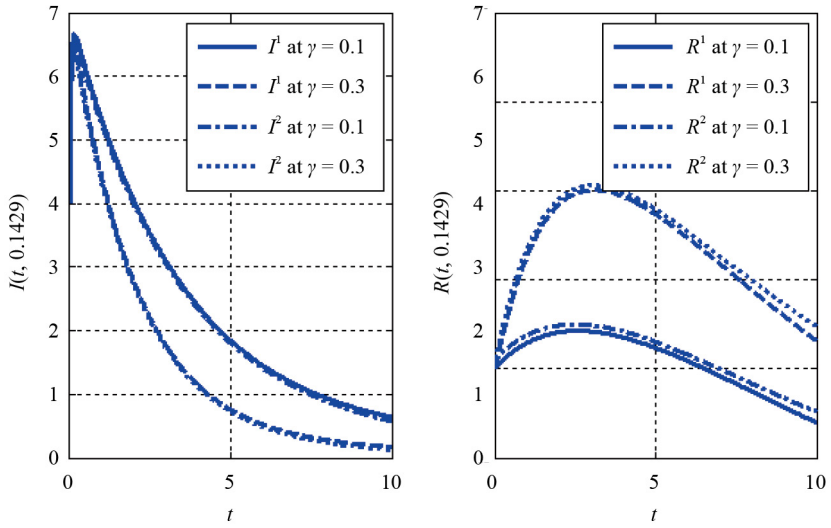

Figure 3. Effect of rate at which infective become recovered to fuzzy infective and recovered people using $d_1 = d_2 = d_3 = d_4 = 0.1$, $\mu = 0.1$, $c_1 = 0.1$, $\Lambda = 0.1$, $\beta_1 = 0.1$, $\theta = 0.1$

In a stochastic fuzzy SIR-β model, Figure 3 shows how the recovery rate γ affects the fuzzy infectious I and recovered R populations. The simulation uses the following parameters: $d_1 = d_2 = d_3 = d_4 = 0.1$, $\mu = 0.1$, $c_1 = 0.1$, $\Lambda = 0.1$, $\beta_1 = 0.1$, $\theta = 0.1$. The two subplots are represented as follows: Left plot: The evolution of the fuzzy infective population I^1 and I^2 over time for different values of γ. The infective population I initially increases and then declines as infected individuals recover or die. A higher recovery rate $\gamma = 0.3$ leads to a faster decline in infective individuals compared to the case with $\gamma = 0.1$. Both the upper bound I^1 and lower bound I^2 of the fuzzy infective population declines faster for $\gamma = 0.3$ than for $\gamma = 0.1$. This is expected because a higher recovery rate means infected individuals recover faster, reducing the pool of active infections. The sharp initial slope of $I(t)$ at $t = 0$ is due to the non-linear infection dynamics and high initial susceptibility, not a singularity. This effect is amplified by stochastic variability and is common in SIR-type models

under rapid disease spread scenarios. Right plot: The evolution of the fuzzy recovered population R^1 and R^2 over time for different values of γ. Over time, the recovered population R grows, reaches a peak, and then stabilizes. A higher recovery rate $\gamma = 0.3$ results in a faster and higher peak of recovered individuals compared to the lower recovery rate $\gamma = 0.1$. The fuzzy upper bound R^1 and lower bound R^2 of the recovered population is higher for $\gamma = 0.3$, showing that more individuals recover in a shorter period. The peak occurs earlier for $\gamma = 0.3$ because individuals recover at a faster rate, but the overall long-term trend shows a stabilization. Increasing recovery rates (e.g., through better treatment, faster diagnosis, and improved healthcare measures) can reduce the spread of the disease by shortening the infectious period. As more individuals recover quickly, the peak of the recovered population is higher and occurs earlier for larger γ.

6.4 *Influence of mortality rate on infective population (Figure 4)*

Figure 4 presents the effect of the mortality rate of the disease θ on the fuzzy infective population I in a stochastic fuzzy SIR-β model. The graph shows how different values of θ influence the upper I^1 and lower I^2 bounds of the infective population over time. The simulation is conducted using the following parameters: $d_1 = d_2 = d_3 = d_4 = 0.1$, $\mu = 0.1$, $\gamma = 0.1$, $c_1 = 0.1$, $\Lambda = 0.1$, $\beta_1 = 0.1$, $\alpha = 0.3$. The infective population initially rises, then declines over time. The faster the decline, the higher the mortality rate θ, as more infected individuals surrender to the disease. The dashed and dotted lines $\theta = 0.3$ show a steeper decline in I^1 and I^2 compared to $\theta = 0.1$. This indicates that a higher disease-induced mortality rate reduces the number of infected individuals more rapidly. The solid and dashed lines represent the upper I^1 and lower I^2 bounds of the fuzzy infective population at $\theta = 0.1$. The dashed and dotted lines represent the corresponding bounds for $\theta = 0.3$. The wider gap between I^1 and I^2 at the start, it gradually narrows, showing greater certainty in the declining trend as the epidemic progresses. A higher mortality rate means more infected individuals die before they can recover, leading to fewer active infections at any given time. If mortality is high, the disease may burn out faster, but at a high human cost. Public health strategies should focus on reducing θ by improving access to treatment and preventing severe infections.

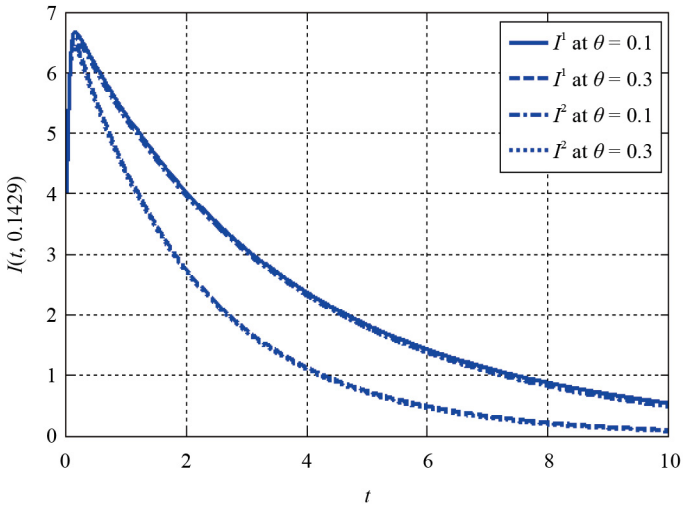

Figure 4. Effect of molarity rate of disease to the fuzzy infective people using $d_1 = d_2 = d_3 = d_4 = 0.1$, $\mu = 0.1$, $\gamma = 0.1$, $c_1 = 0.1$, $\Lambda = 0.1$, $\beta_1 = 0.1$, $\alpha = 0.3$

6.5 *Comparison with existing numerical schemes (Figures 5-8)*

Comparison of the proposed scheme with the existing NSFD scheme for susceptible, infective, recovered populations, and infection rate. The proposed scheme demonstrates better performance, providing solutions closer to those obtained by the MATLAB solver pdepe, which is used as a benchmark in the absence of exact solutions.

Figure 5 compares the proposed two-stage numerical scheme with the Non-Standard Finite Difference (NSFD) scheme for solving the fuzzy susceptible population dynamics in a stochastic fuzzy SIR-β model. The numerical solutions obtained using the NSFD method and the MATLAB solver pdepe are plotted side by side to demonstrate their comparability (left plot). The parameters used in the simulation are: $d_1 = d_2 = d_3 = d_4 = 0.1$, $\mu = 0.1$, $\gamma = 0.03$, $c_1 = 0.1$, $\Lambda = 0.1$, $\beta_1 = 0.1$, $\alpha = 0.1$, $\delta = 0.1$, $\theta = 0.1$. This Figure displays the absolute error between the MATLAB solver pdepe and the NSFD scheme error $\left|S_{pdepe} - S_{NSFD}\right|$. Reaching levels up to 0.5, the number of mistakes is noticeably higher. This implies that the NSFD scheme is less accurate, as it shows greater deviation from the MATLAB solver. Proposed method against MATLAB solver pdepe (right plot). This graphic displays the absolute error between the MATLAB solver pdepe and the proposed scheme error $\left|S_{pdepe} - S_{Proposed}\right|$. At roughly 0.08, the error is rather low. More precisely than the NSFD scheme, the suggested scheme follows the reference solution. Compared to the NSFD system, the proposed one shows far less inaccuracy. The NSFD approach exhibits greater variance, lacking consistency and accuracy across multiple step sizes.

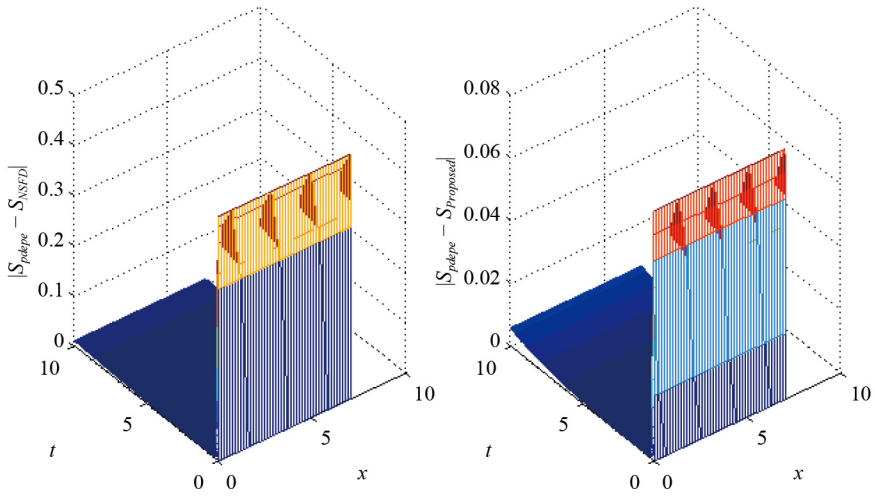

Figure 5. Comparison of proposed and non-standard finite difference scheme for fuzzy susceptible people using $d_1 = d_2 = d_3 = d_4 = 0.1$, $\mu = 0.1$, $\gamma = 0.03$, $c_1 = 0.1$, $\Lambda = 0.1$, $\beta_1 = 0.1$, $\alpha = 0.1$, $\delta = 0.1$, $\theta = 0.1$

Figure 6 compares the Non-Standard Finite Difference (NSFD) scheme for modelling fuzzy infective individuals with the proposed two-stage numerical scheme. The parameters used in the simulation are: $d_1 = d_2 = d_3 = d_4 = 0.1$, $\mu = 0.1$, $\gamma = 0.03$, $c_1 = 0.1$, $\Lambda = 0.1$, $\beta_1 = 0.1$, $\alpha = 0.1$, $\delta = 0.1$, $\theta = 0.1$. The two subplots illustrate the absolute error between the NSFD scheme vs. the MATLAB solver pdepe (left plot). The error is calculated as $\left|I_{pdepe} - I_{NSFD}\right|$, where I_{pdepe} is the reference solution obtained from MATLAB's pdepe solver and I_{NSFD} is the solution using the NSFD scheme. The error is significantly large, reaching values above 1.5. The persistent high error suggests that the NSFD approach fails to yield an accurate solution. This high error suggests that NSFD fails to maintain numerical consistency and stability for the fuzzy infective population. Proposed scheme vs. MATLAB solver pdepe (right plot). The error is calculated as $\left|I_{pdepe} - I_{Proposed}\right|$, where $I_{Proposed}$ is the solution using the proposed scheme. The proposed scheme exhibits much lower error, with a maximum of about 0.08. The error distribution is more controlled, with less deviation over time. This confirms that the proposed scheme is much more accurate and consistent in approximating the fuzzy infective population. The NSFD scheme exhibits significant numerical errors, rendering it unreliable for solving the fuzzy dynamics of infectious populations. The proposed scheme significantly reduces the error, making it a better alternative for solving stochastic fuzzy epidemic models.

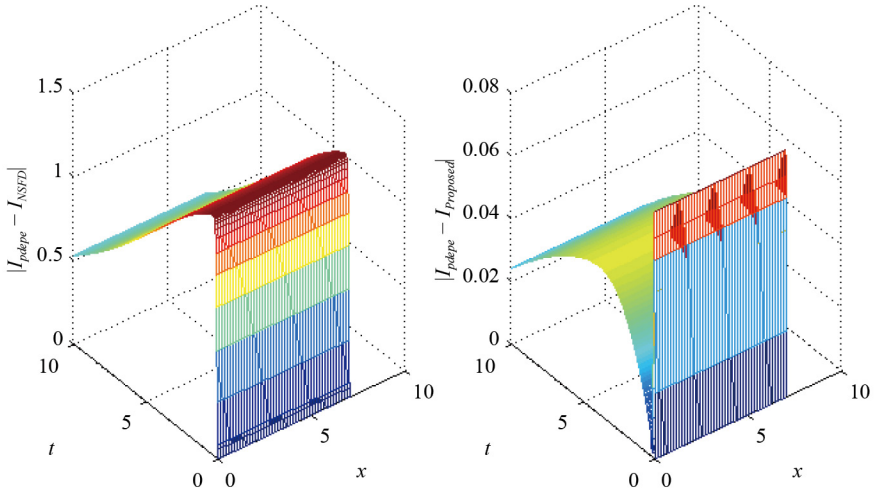

Figure 6. Comparison of proposed and non-standard finite difference scheme for fuzzy infective people using $d_1 = d_2 = d_3 = d_4 = 0.1$, $\mu = 0.1$, $\gamma = 0.03$, $c_1 = 0.1$, $\Lambda = 0.1$, $\beta_1 = 0.1$, $\alpha = 0.1$, $\delta = 0.1$, $\theta = 0.1$

The suggested two-stage numerical method and the Non-Standard Finite Difference (NSFD) strategy for modelling fuzzy recovered individuals R in a stochastic fuzzy $SIR-\beta$ model are compared in Figure 7. The parameters used in the simulation are: $d_1 = d_2 = d_3 = d_4 = 0.1$, $\mu = 0.1$, $\gamma = 0.03$, $c_1 = 0.1$, $\Lambda = 0.1$, $\beta_1 = 0.1$, $\alpha = 0.1$, $\delta = 0.1$, $\theta = 0.1$. The two subplots indicate the absolute inaccuracy between MATLAB solver pdepe (left plot) and the NSFD scheme. Calculated as $\left|R_{pdepe} - R_{NSFD}\right|$ R_{pdepe} is the reference solution from MATLAB's pdepe solver and R_{NSFD} is the solution derived from the NSFD system. The error in the NSFD scheme is significantly large, reaching values above 0.4. The constant high inaccuracy over time points to inadequate numerical accuracy. This implies that the recovered population dynamics cannot be reasonably approximated by the NSFD method. MATLAB solver pdepe compared with the proposed scheme (right plot). Calculated as $\left|R_{pdepe} - R_{Propsed}\right|$, where $R_{Propsed}$ is the solution derived from the suggested numerical method. With a maximum of roughly 0.03, the proposed system generates far less inaccuracy. The more under control the error distribution is, the more precisely the suggested method tracks the MATLAB solver. In approximating the recovered population, the suggested technique shows better numerical stability and precision. Large numerical inaccuracies of the NSFD approach make it unreliable for precisely solving the recovered population dynamics. The suggested method solves the fuzzy SIR-β model with many fewer mistakes, so it is more accurate and consistent.

The proposed two-stage numerical methodology and the Non-Standard Finite Difference (NSFD) method for simulating the fuzzy infection rate β in a stochastic fuzzy SIR-β model are compared in Figure 8. The parameters used in the simulation are: $d_1 = d_2 = d_3 = d_4 = 0.1$, $\mu = 0.1$, $\gamma = 0.03$, $c_1 = 0.1$, $\Lambda = 0.1$, $\beta_1 = 0.1$, $\alpha = 0.1$, $\delta = 0.1$, $\theta = 0.1$. The two subplots indicate the absolute inaccuracy between MATLAB solver pdepe (left plot) and the NSFD scheme. Calculated as $\left|\beta_{pdepe} - \beta_{NSFD}\right|$, where β_{pdepe} is the MATLAB pdepe solver reference solution. The answer derived from the NSFD system is β_{NSFD}. The NSFD scheme has a rather small error, a maximum of about 0.2. The error distribution remains uniform; nonetheless, the NSFD scheme diverges markedly from the reference solution. Proposed scheme vs. MATLAB solver pdepe (right plot). The errors are calculated as: $\left|\beta_{pdepe} - \beta_{Proposed}\right|$, where $\beta_{Proposed}$ is the solution obtained using the proposed numerical scheme. The proposed scheme has a slightly higher error, reaching around 0.5. The error distribution follows a consistent trend but shows greater deviation than the NSFD scheme. Unlike previous comparisons where the proposed scheme performed better, this suggests that the NSFD scheme approximates the fuzzy infection rate β slightly more accurately than the proposed scheme. Unlike earlier Figures, where the proposed scheme significantly outperformed the NSFD scheme, this Figure suggests that NSFD provides a better approximation for the infection rate β. The proposed scheme maintains numerical stability but introduces a slightly larger error for β. This indicates that additional refinements may be needed in the proposed scheme better to capture the dynamic nature of the infection rate.

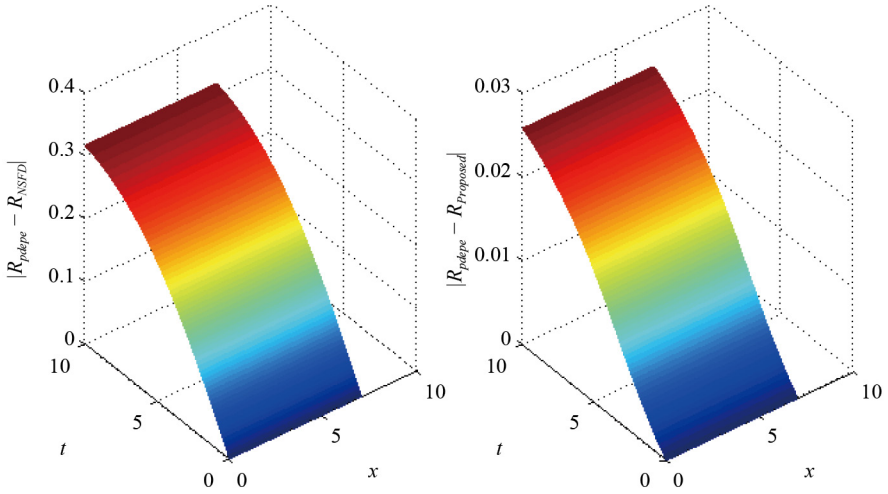

Figure 7. Comparison of proposed and non-standard finite difference scheme for fuzzy recovered people using $d_1 = d_2 = d_3 = d_4 = 0.1$, $\mu = 0.1$, $\gamma = 0.03$, $c_1 = 0.1$, $\Lambda = 0.1$, $\beta_1 = 0.1$, $\alpha = 0.1$, $\delta = 0.1$, $\theta = 0.1$

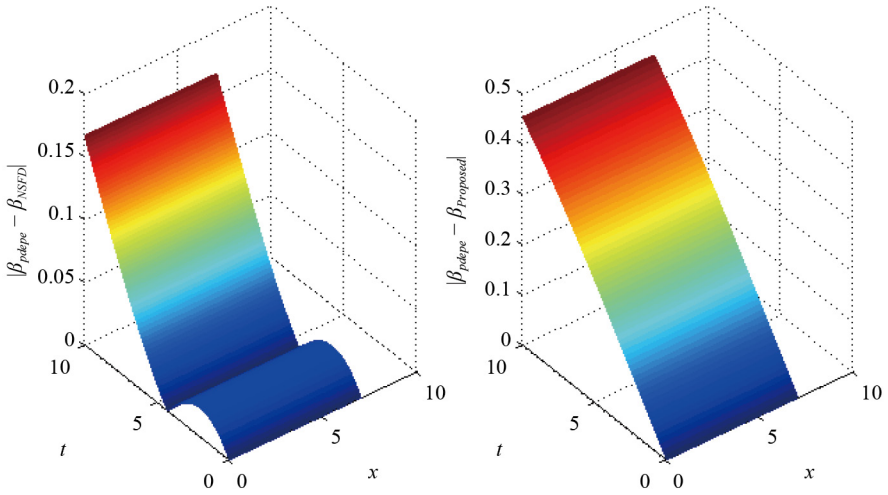

Figure 8. Comparison of proposed and non-standard finite difference scheme for fuzzy infection rate using $d_1 = d_2 = d_3 = d_4 = 0.1$, $\mu = 0.1$, $\gamma = 0.03$, $c_1 = 0.1$, $\Lambda = 0.1$, $\beta_1 = 0.1$, $\alpha = 0.1$, $\delta = 0.1$, $\theta = 0.1$

As noted in [64], the non-standard finite difference method lacks first-order temporal accuracy and is inconsistent for any selected step size. Given that the exact solution to the problem is unknown, the solution obtained by the Matlab solver pdepe is used as a substitute. The MATLAB solver can solve some partial differential equations. The problem can be addressed using the pdepe solver; thus, the numerical solution derived from this solver is employed for comparative analysis. The proposed technique yields results that are generally closer to the solver's answer in most instances.

6.6 *Clarification on the use of MATLAB's PDE solver as a reference*

It is important to note that the MATLAB solver is used here as a reference baseline, not as a competitor to our proposed scheme, because it provides numerical approximations to deterministic PDEs only, does not support stochasticity, and cannot handle fuzzy parameters. Therefore, the MATLAB solver is used only in the deterministic setup (with crisp parameters) to assess how closely the proposed scheme matches solutions from a highly validated numerical engine. It

is not an alternative or substitute in cases involving fuzziness, randomness, or their combination, which are the primary challenges this study addresses.

6.7 *Why the proposed scheme is needed despite MATLAB solver accuracy*

The proposed scheme is designed specifically for fuzzy stochastic PDEs, where standard tools like pdepe are inapplicable or fail to converge. It is second-order accurate in time for deterministic problems, and mean-square stable for stochastic models, outperforming the first-order NSFD and Euler-Maruyama methods in most tested scenarios. It also provides greater flexibility, including handling interval uncertainty (fuzziness) via the β-cut formulation, modelling random fluctuations through a stochastic component, and using a compact spatial discretization that increases spatial accuracy without requiring dense grids.

6.8 *Comparison of numerical solutions for different time steps*

Figure 9 shows the sensitivity of the proposed numerical scheme to different time step sizes Δt. Figure 9 also illustrates how the solution evolves when using different time step sizes: $\Delta t = 0.1$, 0.05, and $\Delta t = 0.01$. The proposed scheme shows consistent and stable behaviour across all tested Δt values, with higher resolution (smaller Δt) offering finer solution accuracy, but $\Delta t = 0.1$ already captures the core dynamics effectively.

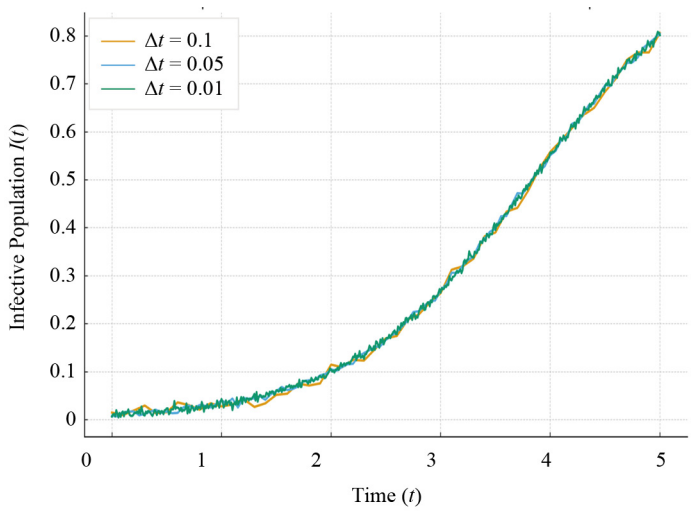

Figure 9. Comparison of infective population $I(t)$ for varying $\Delta t = 0.1$, 0.05, 0.01 values

7. Conclusion

In this research, we have developed a novel computational scheme tailored for the fuzzy stochastic SIR-β model with diffusion, addressing the complexities inherent in modelling infectious disease dynamics under uncertainty and spatial considerations. Our scheme's two-level construction eliminates the need for auxiliary methods at the initial time step, simplifying the computational process. While the modified exponential integrator improves stability by effectively handling stiff equations, the integrated compact spatial discretization enhances computational accuracy and efficiency. Using a comprehensive analysis of its mean-square stability and consistency, we confirmed the method's reliability for practical use. We tested the efficiency of our technique against pre-existing non-standard finite difference methods using the stochastic fuzzy diffusive SIR-β model.

In most cases, our proposed scheme beats the competition and shows promise as a strong tool for simulating complex epidemic dynamics. Find solutions to partial differential equations using the Matlab solver pdepe; thereafter, you can evaluate the results of the two approaches. The concluding remarks may be expressed as:

• The proposed numerical scheme consistently outperforms the existing NSFD method, demonstrating higher accuracy and improved stability across most test scenarios.

• The simulation results show that increasing population resistance or adaptive social behaviour leads to a noticeable decline in both the lower and upper bounds of the fuzzy infection rate, indicating reduced transmission potential.

• Enhancing the molarity (disease-induced mortality) rate results in a significant decrease in both fuzzy components of the infective population, reflecting a faster reduction in active infections within the modelled system.

The advancements presented in this study contribute to computational epidemiology by providing a more accurate and efficient method for simulating the spread of infectious diseases under uncertainty. Future research could involve applying this computational framework to real events and extending it across several epidemiological models to assess its broader applicability.

Limitations Absence of Empirical Data Fitting: While the current study does not fit the model to real-world data, the focus is on developing and validating a robust numerical scheme that can handle highly complex epidemic dynamics involving fuzziness, nonlinearity, and stochasticity simultaneously. Future work will focus on parameter calibration using real epidemic datasets, particularly COVID-19 and influenza, where uncertainty and noise are prevalent. However, even without direct data fitting, the simulations qualitatively demonstrate plausible dynamic behaviours across different parameter regimes (e.g., resistance to social behaviour, varying recovery rates, and disease mortality).

Broader Applicability without Data: The proposed model, despite not being fitted to data, is valuable for: Demonstrating the influence of uncertainty and randomness in a controlled simulation environment, benchmarking numerical schemes capable of capturing nonlinearity and uncertainty and serving as a template model for future calibration to real datasets with inherent fuzziness and stochasticity.

Author contributions

Conceptualization, methodology, and analysis, Y.N.; funding acquisition, M.S.A.; investigation, M.S.A.; methodology, Y.N.; project administration, M.S.A.; resources, M.S.A.; supervision, M.S.A.; visualization, M.S.A.; writing review and editing, M.S.A.; proofreading and editing, Y.N. All authors have read and agreed to the published version of the manuscript.

Funding

The authors would like to acknowledge the support of Prince Sultan University for paying the Article Processing Charges of this publication.

Data availability statement

The manuscript included all required data and the implementation of information.

Acknowledgments

The authors wish to express their gratitude to Prince Sultan University for facilitating the publication of this article through the Theoretical and Applied Sciences Lab.

Confilict of interest

The authors declare no competing financial interest.

References

[1] Lessler J, Cummings DA. Mechanistic models of infectious disease and their impact on public health. *American Journal of Epidemiology*. 2016; 183(5): 415-422. Available from: https://doi.org/10.1093/aje/kww021.

[2] Huo J, Zhao H, Zhu L. The effect of vaccines on backwards bifurcation in a fractional order HIV model. *Nonlinear Analysis: Real World Applications*. 2015; 26: 289-305. Available from: https://doi.org/10.1016/J.NONRWA.2015.05.014.

[3] Mandal S, Sarkar RR, Sinha S. Mathematical models of malaria—a review. *Malaria Journal*. 2011; 10(1): 202. Available from: https://doi.org/10.1186/1475-2875-10-202.

[4] Bernoulli D, Blower S. An attempt at a new analysis of the mortality caused by smallpox and of the advantages of inoculation to prevent it. *Reviews in Medical Virology*. 2004; 14(5): 275-288. Available from: https://doi.org/10.1002/rmv.443.

[5] Kermack WO, McKendrick AG. A contribution to the mathematical theory of epidemics. *Proceedings of the Royal Society of London Series A, Containing Papers of a Mathematical and Physical Character*. 1927; 115(772): 700-721. Available from: https://doi.org/10.1098/rspa.1927.0118.

[6] Kermack WO, McKendrick AG. Contributions to the mathematical theory of epidemics. II. The problem of endemicity. *Proceedings of the Royal Society of London Series A, Containing Papers of a Mathematical and Physical Character*. 1932; 138(834): 55-83. Available from: https://doi.org/10.1098/rspa.1932.0171.

[7] Kermack WO, McKendrick AG. Contributions to the mathematical theory of epidemics. Part III. *Proceedings of the Royal Society of London Series B, Containing Papers of a Biological Character*. 1933; 141: 94-112. Available from: http://www.jstor.org/stable/96207.

[8] En'ko PD. On the course of epidemics of some infectious diseases. *International Journal of Epidemiology*. 1989; 18(4): 749-755. Available from: https://doi.org/10.1093/ije/18.4.749.

[9] Olopade AI, Adesanya AO, Akinwumi TO. Mathematical transmission of SEIR epidemic model with natural immunity. *Asian Journal of Pure and Applied Mathematics*. 2021; 3(1): 19-29.

[10] Mossong J, Muller CP. Modelling measles re-emergence as a result of waning of immunity in vaccinated populations. *Vaccine*. 2003; 21(31): 4597-4603. Available from: https://doi.org/10.1016/s0264-410x(03)00449-3.

[11] Leuridan E, van Damme P. Passive transmission and persistence of naturally acquired or vaccine-induced maternal antibodies against measles in newborns. *Vaccine*. 2007; 25(34): 6296-6304. Available from: https://doi.org/10.1016/j.vaccine.2007.05.030.

[12] Scherer A, McLean A. Mathematical models of vaccination. *British Medical Bulletin*. 2002; 62(1): 187-199. Available from: https://doi.org/10.1093/bmb/62.1.187.

[13] Sanches RP, Ferreira CP, Kraenkel RA. The role of immunity and seasonality in cholera epidemics. *Bulletin of Mathematical Biology*. 2011; 73(12): 2916-2931. Available from: https://doi.org/10.1007/s11538-011-9652-6.

[14] Jain S, Kumar S. Dynamic analysis of the role of innate immunity in SEIS epidemic model. *European Physical Journal Plus*. 2021; 136(4): 439. Available from: https://doi.org/10.1140/epjp/s13360-021-01390-3.

[15] Zadeh LA. Fuzzy sets. *Information and Control*. 1965; 8(3): 338-353. Available from: https://doi.org/10.1016/S0019-9958(65)90241-X.

[16] Barros LC, Leite MBF, Bassanezi RC. The SI epidemiological models with a fuzzy transmission parameter. *Computers & Mathematics with Applications*. 2003; 45(11): 1619-1628. Available from: https://doi.org/10.1016/S0898-1221(03)00141-X.

[17] Mondal PK, Jana S, Haldar P, Kar TK. Dynamical behavior of an epidemic model in a fuzzy transmission. *International Journal of Uncertainty, Fuzziness and Knowledge-Based Systems*. 2015; 23(5): 651-665. Available from: https://doi.org/10.1142/S0218488515500282.

[18] Mishra BK, Pandey SK. Fuzzy epidemic model for the transmission of worms in computer network. *Nonlinear Analysis: Real World Applications*. 2010; 11(5): 4335-4341. Available from: https://doi.org/10.1016/j.nonrwa.2010.05.018.

[19] Mickens RE. Dynamic consistency: a fundamental principle for constructing nonstandard finite difference schemes for differential equations. *Journal of Difference Equations and Applications*. 2005; 11(7): 645-653. Available from: https://doi.org/10.1080/10236190412331334527.

[20] Verma AK, Kayenat S. An efficient Mickens' type NSFD scheme for the generalized Burgers-Huxley equation. *Journal of Difference Equations and Applications*. 2020; 26(9-10): 1213-1246. Available from: https://doi.org/10.1080/10236198.2020.1812594.

[21] Khalsaraei MM, Shokri A, Ramos H, Heydari S. A positive and elementary stable non-standard explicit scheme for a mathematical model of the influenza disease. *Mathematics and Computers in Simulation*. 2021; 182: 397-410. Available from: https://doi.org/10.1016/j.matcom.2020.11.013.

[22] Raza A, Rafiq M, Baleanu D, Arif MS, Naveed M, Ashraf K. Competitive numerical analysis for stochastic HIV/AIDS epidemic model in a two-sex population. *IET Systems Biology*. 2019; 13(6): 305-315. Available from: https://doi.org/10.1049/iet-syb.2019.0051.

[23] Jawaz M, Ahmed N, Baleanu D, Rafiq M, Rehman MA. Positivity preserving technique for the solution of HIV/AIDS reaction diffusion model with time delay. *Frontiers in Physics*. 2020; 7: 483. Available from: https://doi.org/10.3389/fphy.2019.00229.

[24] Cresson J, Pierret F. Non-standard finite difference schemes preserving dynamical properties. *Journal of Computational and Applied Mathematics*. 2016; 303: 15-30. Available from: https://doi.org/10.1016/j.cam.2016.02.007.

[25] Baleanu D, Zibaei S, Namjoo M, Jajarmi A. A non-standard finite difference scheme for the modeling and nonidentical synchronization of a novel fractional chaotic system. *Advances in Difference Equations*. 2021; 2021(1): 308. Available from: https://doi.org/10.1186/s13662-021-03454-1.

[26] Baazeem AS, Nawaz Y, Arif MS, Abodayeh K, AlHamrani MA. Modelling infectious disease dynamics: a robust computational approach for stochastic SIRS with partial immunity and an incidence rate. *Mathematics*. 2023; 11(23): 4794. Available from: https://doi.org/10.3390/math11234794.

[27] Arif MS, Abodayeh K, Nawaz Y. Precision in disease dynamics: finite difference solutions for stochastic epidemics with treatment cure and partial immunity. *Partial Differential Equations in Applied Mathematics*. 2024; 9: 100660. Available from: https://doi.org/10.1016/j.padiff.2024.100660.

[28] Arif MS, Abodayeh K, Nawaz Y. Numerical modeling of mixed convective nanofluid flow with fractal stochastic heat and mass transfer using finite differences. *Frontiers in Energy Research*. 2024; 12: 1373079. Available from: https://doi.org/10.3389/fenrg.2024.1373079.

[29] Aslefallah M, Yuzbasi S, Abbasbandy S. A numerical investigation based on exponential collocation method for non-linear SITR model of COVID-19. *Computer Modeling in Engineering & Sciences*. 2023; 136(2): 1687-1706. Available from: https://doi.org/10.32604/cmes.2023.025647.

[30] Aslefallah M, Abbasbandy S, Shivanian E. Numerical solution of a modified anomalous diffusion equation with non-linear source term through meshless singular boundary method. *Engineering Analysis with Boundary Elements*. 2019; 107: 198-207. Available from: https://doi.org/10.1016/j.enganabound.2019.07.016.

[31] Aslefallah M, Rostamy D. Application of the singular boundary method to the two-dimensional telegraph equation on arbitrary domains. *Journal of Engineering Mathematics*. 2019; 118(1): 1-14. Available from: https://doi.org/10.1007/s10665-019-10008-8.

[32] Shivanian E, Aslefallah M. Stability and convergence of spectral radial point interpolation method locally applied on two dimensional pseudo-parabolic equation. *Numerical Methods for Partial Differential Equations*. 2017; 33(3): 724-741. Available from: https://doi.org/10.1002/num.22119.

[33] Allehiany FM, Dayan F, Al-Harbi FF, Althobaiti N, Ahmed N, Rafiq M, et al. Bio-inspired numerical analysis of COVID-19 with fuzzy parameters. *Computers, Materials & Continua*. 2022; 72(2): 3213-3229. Available from: https://doi.org/10.32604/cmc.2022.025811.

[34] Alhebshi RM, Ahmed N, Baleanu D, Fatima U, Dayan F, Rafiq M, et al. Modeling of computer virus propagation with fuzzy parameters. *Computers, Materials & Continua*. 2023; 74(3): 5663-5678. Available from: https://doi.org/10.32604/cmc.2023.033319.

[35] Chatterjee K, Chatterjee K, Kumar A, Shankar S. Healthcare impact of COVID-19 epidemic in India: a stochastic mathematical model. *Medical Journal Armed Forces India*. 2020; 76(2): 147-155. Available from: https://doi.org/10.1016/j.mjafi.2020.03.022.

[36] Funk S, Camacho A, Kucharski AJ, Eggo RM, Edmunds WJ. Real-time forecasting of infectious disease dynamics with a stochastic semi-mechanistic model. *Epidemics*. 2018; 22: 56-61. Available from: https://doi.org/10.1016/j.epidem.2016.11.003.

[37] Gao N, Song Y, Wang X, Liu J. Dynamics of a stochastic SIS epidemic model with non-linear incidence rates. *Advances in Difference Equations*. 2019; 2019(1): 1. Available from: https://doi.org/10.1186/s13662-019-1980-0.

[38] Song Y, Miao A, Zhang T, Wang X, Liu J. Extinction and persistence of a stochastic SIRS epidemic model with saturated incidence rate and transfer from infectious to susceptible. *Advances in Difference Equations*. 2018; 2018(1): 293. Available from: https://doi.org/10.1186/s13662-018-1759-8.

[39] Miao A, Wang X, Zhang T, Wang W, Sampath Aruna Pradeep BG. Dynamical analysis of a stochastic SIS epidemic model with non-linear incidence rate and double epidemic hypothesis. *Advances in Difference Equations*. 2017; 2017(1): 226. Available from: https://doi.org/10.1186/s13662-017-1289-9.

[40] Cai Y, Jiao J, Gui Z, Liu Y, Wang W. Environmental variability in a stochastic epidemic model. *Applied Mathematics and Computation*. 2018; 329: 210-226. Available from: https://doi.org/10.1016/j.amc.2018.02.009.

[41] Meng X, Li F, Gao S. Global analysis and numerical simulations of a novel stochastic eco-epidemiological model with time delay. *Applied Mathematics and Computation*. 2018; 339: 701-726. Available from: https://doi.org/10.1016/j.amc.2018.07.039.

[42] Khan T, Khan A, Zaman G. The extinction and persistence of the stochastic hepatitis B epidemic model. *Chaos, Solitons & Fractals*. 2018; 108: 123-128. Available from: https://doi.org/10.1016/j.chaos.2018.01.036.

[43] Chen X, Li J, Xiao C, Yang P. Numerical solution and parameter estimation for uncertain SIR model with application to COVID-19. *Fuzzy Optimization and Decision Making*. 2021; 20(2): 189-208. Available from: https://doi.org/10.1007/s10700-020-09342-9.

[44] Baber MZ, Seadway AR, Iqbal MS, Ahmed N, Yasin MW, Ahmed MO. Comparative analysis of numerical and newly constructed soliton solutions of stochastic Fisher-type equations in a sufficiently long habitat. *International Journal of Modern Physics B*. 2022; 37(12): 2350155. Available from: https://doi.org/10.1142/S0217979223501552.

[45] Zhao M, Zhao H. Asymptotic behavior of global positive solution to a stochastic SIR model incorporating media coverage. *Advances in Difference Equations*. 2016; 2016(1): 149. Available from: https://doi.org/10.1186/s13662-016-0884-5.

[46] El-Borai MM, Moustafa OL, Ahmed HM. Asymptotic stability of some stochastic evolution equations. *Applied Mathematics and Computation*. 2003; 144(2-3): 273-286. Available from: https://doi.org/10.1016/S0096-3003(02)00406-X.

[47] Ahmed HM. Controllability of impulsive neutral stochastic differential equations with fractional Brownian motion. *IMA Journal of Mathematical Control and Information*. 2015; 32(4): 781-794. Available from: https://doi.org/10.1093/imamci/dnu019.

[48] Ahmed AS, Ahmed HM, Nofal TA, Darwish A, Omar OA. Hilfer-Katugampola fractional epidemic model for malware propagation with optimal control. *Ain Shams Engineering Journal*. 2024; 15(10): 102945. Available from: https://doi.org/10.1016/j.asej.2024.102945.

[49] Capasso V, Serio G. A generalization of the Kermack-McKendrick deterministic epidemic model. *Mathematical Biosciences*. 1978; 42: 43-61. Available from: https://doi.org/10.1016/0025-5564(78)90006-8.

[50] Kolokolnikov T, Iron D. Law of mass action and saturation in SIR model with application to coronavirus modelling. *Infectious Disease Modelling*. 2021; 6: 91-97. Available from: https://doi.org/10.1016/j.idm.2020.11.002.

[51] Liu R, Wu J, Zhu H. Media/psychological impact on multiple outbreaks of emerging infectious diseases. *Computational and Mathematical Methods in Medicine*. 2007; 8(3): 153-164. Available from: https://doi.org/10.1080/17486700701425870.

[52] Xiao Y, Tang S, Wu J. Media impact switching surface during an infectious disease outbreak. *Scientific Reports*. 2015; 5: 7838. Available from: https://doi.org/10.1038/srep07838.

[53] Cui J, Sun Y, Zhu H. The impact of media on the control of infectious diseases. *Journal of Dynamics and Differential Equations*. 2008; 20: 31-53. Available from: https://doi.org/10.1007/s10884-007-9075-0.

[54] Mani G, Elangovan P, Martin J, Thabet S, Kedim I, Abdeljawad T. Mathematical modeling and analysis of COVID-19 transmission dynamics via Caputo-Fabrizio fractional operator. *Fractals*. 2025; 33(5): 2450216. Available from: https://doi.org/10.1142/S0218348X25501300.

[55] Selvam A, Sabarinathan S, Khan H, Alzabut J, Gómez-Aguilar JF. Numerical simulation of Ebola transmission disease dynamics using fractional derivatives involving real data for more effective prediction. *International Journal of Modeling, Simulation, and Scientific Computing*. 2025; 16(5): 1. Available from: https://doi.org/10.1142/S179396232550062X.

[56] Bansal J, Kumar A, Kumar A, Khan A, Abdeljawad T. Investigation of monkeypox disease transmission with vaccination effects using fractional order mathematical model under Atangana-Baleanu Caputo derivative. *Modeling Earth Systems and Environment*. 2025; 11(1): 40. Available from: https://doi.org/10.1007/s40808-024-02202-0.

[57] Baazeem A, Arif M, Nawaz Y, Abodayeh K. Modeling and simulation of epidemics using q-diffusion-based SEIR framework with stochastic perturbations. *Computer Modeling in Engineering & Sciences*. 2025; 143(3): 3463. Available from: https://doi.org/10.32604/cmes.2025.066299.

[58] Arif MS, Abodayeh K, Nawaz Y. A hybrid finite difference approach for solving fuzzy stochastic SIR-β model with diffusion and incidence rate. *European Journal of Pure and Applied Mathematics*. 2025; 18(3): 6292. Available from: https://doi.org/10.29020/nybg.ejpam.v18i3.6292.

[59] Arif MS, Abodayeh K, Nawaz Y. A hybrid exponential Runge-Kutta scheme for stochastic SIQR disease modeling. *European Journal of Pure and Applied Mathematics*. 2025; 18(3): 6176. Available from: https://doi.org/10.29020/nybg.ejpam.v18i3.6176.

[60] Buonomo B, Della Marca R, Sharbayta SS. A behavioral change model to assess vaccination-induced relaxation of social distancing during an epidemic. *Journal of Biological Systems*. 2022; 30(1): 1-25. Available from: https://doi.org/10.1142/S0218339022500085.

[61] Wang X, Zhang S. Coupling media coverage and susceptibility for modeling epidemic dynamics: An application to COVID-19. *Mathematics and Computers in Simulation*. 2024; 217: 374-394. Available from: https://doi.org/10.1016/j.matcom.2023.10.026.

[62] Bulai IM, Montefusco F, Pedersen MG. Stability analysis of a model of epidemic dynamics with non-linear feedback producing recurrent infection waves. *Applied Mathematics Letters*. 2023; 136: 108455. Available from: https://doi.org/10.1016/j.aml.2022.108455.

[63] Bartwal P, Upreti H, Pandey AK, Joshi N, Joshi BP. Application of modified Fourier's law in a fuzzy environment to explore the tangent hyperbolic fluid flow over a non-flat stretched sheet using the LWCM approach. *International Communications in Heat and Mass Transfer*. 2024; 153: 107332. Available from: https://doi.org/10.1016/j.icheatmasstransfer.2024.107332.

[64] Pasha SA, Nawaz Y, Arif MS. On the non-standard finite difference method for reaction-diffusion models. *Chaos, Solitons & Fractals*. 2023; 166: 112929. Available from: https://doi.org/10.1016/j.chaos.2022.112929.